

T. GROTDAL, K. NYBØ AND B. ELBEK

A STUDY OF ENERGY LEVELS IN
ODD-MASS DYSPROSIUM NUCLEI
BY MEANS OF
(*d,p*) AND (*d,t*) REACTIONS

Det Kongelige Danske Videnskabernes Selskab
Matematisk-fysiske Meddelelser **37**, 12



Kommissionær: Munksgaard
København 1970

CONTENTS

	Pages
1. Introduction	3
2. Results and Discussion	4
2.1. Q -values and Neutron Separation Energies	4
2.2. General Features of the Spectra	4
2.3. Detailed Interpretation of the Spectra	5
2.3.1. The $3/2 - [521]$ Orbital	9
2.3.2. The $1/2 + [660]$, $3/2 + [651]$ and $5/2 + [642]$ Orbitals	16
2.3.3. The $3/2 + [402]$ Orbital	25
2.3.4. The $1/2 + [400]$ Orbital	31
2.3.5. The $11/2 - [505]$ Orbital	33
2.3.6. The $3/2 - [532]$ Orbital	35
2.3.7. The $1/2 - [530]$ Orbital	35
2.3.8. The $7/2 + [404]$ Orbital	38
2.3.9. The $5/2 - [523]$ Orbital	38
2.3.10. The $7/2 + [633]$ Orbital	40
2.3.11. The $1/2 - [521]$ Orbital	40
2.3.12. The $5/2 - [512]$ Orbital	43
2.3.13. The $1/2 - [510]$ Orbital	43
2.3.14. The $3/2 - [512]$ Orbital	45
3. Z -dependence of Single-Quasiparticle Energies	46
4. Summary	50
References	51

Synopsis

The energy levels of ^{155}Dy , ^{157}Dy , ^{159}Dy , ^{161}Dy , ^{163}Dy , and ^{165}Dy have been investigated by means of (d,p) and (d,t) reactions. The deuteron energy was 12.1 MeV and the charged reaction products were analyzed in a magnetic spectrograph at angles of observation of 60° , 90° , and 125° . A total of 16 Nilsson orbitals or components thereof were identified on the basis of total cross sections and the intensity patterns for the rotational states. Comparison of the experimental cross sections with those predicted on the basis of DWBA calculations and theoretical wave functions allowed an estimate of the single-particle components in the excited states. Some dependence of the neutron level density on the proton number is evident from comparison with the data for the isotopes of Gd and Er.

1. Introduction

The present study of the energy levels in the odd dysprosium isotopes by means of neutron stripping and pick-up reactions is a continuation of earlier investigations of the energy levels in odd gadolinium¹⁾, erbium²⁾, and ytterbium³⁾ nuclei.

As in the earlier experiments, the main result of this type of study is the systematic localization of a large number of neutron single-particle states. The relative simplicity of the spectrum analysis permits localization of such states over a considerably wider span of energy than is generally investigated in decay scheme work. Thus, most of the energy levels below 1 MeV of excitation, which are populated in the neutron transfer reactions, can be given a rather definite single-neutron assignment. At higher energies of excitation, only strong single-particle components can be identified, but it should be noted that, also at lower excitation energies, especially in neutron-deficient nuclei, strong couplings of the various modes of excitation give rise to complicated level structures which as yet have been only partially analyzed.

The level structures of several of the dysprosium isotopes have earlier been subject to a number of decay scheme and reaction studies. Thus, ¹⁵⁹Dy has been investigated by BORGGREEN et al.⁴⁾ and ¹⁶¹Dy by FUNKE et al.⁵⁾. The latter authors have also investigated the ¹⁶³Dy levels, which furthermore have been studied very completely by SCHULT et al.⁶⁾ who used a number of different nuclear reactions including the (*d,p*) and (*d,t*) reactions. Finally, the ¹⁶⁵Dy levels have been investigated by several groups⁷⁻¹⁰⁾. The results of these former studies have been of great importance for many of the conclusions drawn in the present work. Additional information about ¹⁶¹Dy and ¹⁶³Dy was obtained from inelastic deuteron scattering spectra recorded separately¹¹⁾.

The experimental methods used were the same as those in the earlier investigations¹⁻³⁾. The beam of 12.1 MeV deuterons was obtained from the Niels Bohr Institute tandem accelerator and the charged reaction products

were analyzed in a broad range magnetic spectrograph with photographic plate recording. The targets for the investigation were $\sim 40 \mu\text{g}/\text{cm}^2$ layers of the isotopes directly deposited on $\sim 40 \mu\text{g}/\text{cm}^2$ carbon foils in the electromagnetic isotope separator at the University of Aarhus.

Absolute spectroscopic factors were obtained from the observed cross sections by comparison with the results of distorted wave Born approximation calculations (DWBA). The calculated cross sections for the dysprosium nuclei were actually the averages of those used for gadolinium¹⁾ and erbium²⁾ and thus suffer from the same deficiencies as discussed before²⁾. The DWBA single-particle cross sections $\sigma_l(\theta)$, defined as in ref. 1, were calculated for a (d,p) Q -value of $+3$ MeV and a (d,t) Q -value of -2 MeV. These Q -values are used as reference values to which all experimental cross sections were reduced before comparison with the theoretical cross sections.

2. Results and Discussion

A spectrum is shown in Figs. 1–10 for each of the ten different transfer reactions possible with the stable targets ^{156}Dy , ^{158}Dy , ^{160}Dy , ^{162}Dy , and ^{164}Dy . The average level energies and the differential cross sections are listed in Tables 1–6, which also contain the suggested Nilsson assignments for some of the levels. The basis for these assignments will be discussed in detail in the following sections.

2.1. Q -values and Neutron Separation Energies

The ground-state group was easily localized in all the spectra and the ground-state Q -values for the (d,p) and (d,t) reactions were therefore obtained in a straightforward manner. The spectrograph calibration was based on the 6.0498 MeV and 8.7864 MeV α -groups from ^{212}Bi and ^{212}Po , respectively. The Q -values are listed in Table 7 together with the corresponding neutron separation energies. Comparison with the 1964 Mass Table¹²⁾ reveals considerable deviations especially for the neutron-deficient isotopes. The agreement with the (d,p) Q -values from the Florida group is satisfactory^{6, 7)}.

2.2. General Features of the Spectra

The analysis of the neutron transfer spectra for the dysprosium isotopes was greatly facilitated by the previous analysis of the spectra for the isotopes in the Gd and Er series of isotopes^{1, 2)}. There is a considerable regularity

TABLE 1. Levels populated in ^{155}Dy .

Energy average (d,t) keV	Assignment	$d\sigma/d\Omega(d,t)$ $\mu\text{b/sr}$		
		60°	90°	125°
0	3/2 3/2 - [521]	46	41	25
86	3/2 3/2 + [651] (+ 3/2 + [402])	76	105	67
134	7/2 3/2 - [521]	36	49	34
153	11/2 11/2 - [505]	7	17	16
201		6	5	3
223	9/2 3/2 - [521]	6	13	15
239	3/2 3/2 + [402] (+ 3/2 + [651])	115	170	149
320	1/2 1/2 + [400]	109	166	126
345		13	16	12
381	3/2 1/2 - [530]	46	55	35
422	5/2 1/2 - [530]	6	10	9
445		11	10	9
457		4	4	3
482	7/2 1/2 - [530]	12	20	-

in the change of properties of the various single-particle states and, in most cases, the properties deduced for the Dy nuclei are intermediate of those found for Gd and Er.

Among the more striking regularities is a shift of the energy levels for a given neutron number as the proton number is increased. This is illustrated in Figs. 21-22.

In spite of the strong low-lying collective excitations in the even nuclei, the energy spectra for the odd Dy nuclei are not more complex than those for the odd Gd nuclei.

Some information about the collective levels connected by large matrix elements to the ground states in ^{161}Dy or ^{163}Dy was obtained in a concurrent⁽¹¹⁾ study of the inelastic deuteron scattering from these nuclei. These data have not yet been finally analyzed, but have nevertheless given supporting evidence for several of the assignments discussed in detail in the following sections.

2.3. Detailed Interpretation of the Spectra

The assignments of the single-neutron orbitals are least ambiguous near the ground states and, consequently, the analysis proceeds from the ground states towards deeper hole states by means of the (d,t) spectra and then from the ground states towards higher particle states by means of the (d,p)

TABLE 2. Levels populated in ^{157}Dy .

Energy average		Assignment	$d\sigma/d\Omega(d,p) \text{ } \mu\text{b/sr}$			$d\sigma/d\Omega(d,t) \text{ } \mu\text{b/sr}$		
(d,p) keV	(d,t) keV		60°	90°	125°	60°	90°	125°
0	0	3/2 3/2 - [521]	86	35	12	56	55	26
59	61	5/2 3/2 - [521]	3	2	1	0.6	0.6	0.4
147	147	7/2 3/2 - [521]	196	96	41	69	96	46
161	161	9/2 +	70	44	17	43	67	34
	187					6	7	4
198	198	11/2 11/2 - [505]	27	10	9	12	30	33
	209					2	9	2
235	235	3/2 3/2 + [651] + 3/2 + [402]	95	74	47	87	153	94
254	257	9/2 3/2 - [521]	19	17	13	5	9	7
306	307	3/2 3/2 + [402] + 3/2 + [651]	43	25	13	86	146	97
339	340	5/2 5/2 - [523]	42	26	14	13	19	14
	350	13/2 +				14	17	7
387	388	1/2 1/2 + [400]	121	44	24	167	283	178
	399	3/2 3/2 - [532]				11	22	8
416	418	7/2 5/2 - [523]	164	99	50	19	30	15
	432					9	17	13
	454	5/2 3/2 - [532]				7	20	12
463	464	1/2 1/2 - [521]	206	102	38	26	34	14
	506					14	24	13
520	517	3/2 1/2 - [521], 9/2 5/2 - [523]	48	36	18	23	40	31
	527	7/2 3/2 - [532]				8	16	11
553	555	5/2 1/2 - [521], 3/2 1/2 - [530]	176	89	38	99	138	68
565	565	5/2 1/2 - [530]	16	23	6	16	16	6
607			32	20	8			
670	673	7/2 1/2 - [521], 7/2 1/2 - [530]	47	32	17	18	27	18
	685					2	4	2
704			2	2	1			
	712					2	3	2
728	731		32	22	12	6	10	10
752	756		18	6	2	7	8	4
768	770		22	18	11	3	6	2
785			4	6	3			
823	828		4	3	1		2	1
863			2	2	2			
881			30	18	5			
901			4	5	2			
934			12	9	4			
965			5	5	2			
985		7/2 5/2 - [512]	70	55	22			

(continued)

TABLE 2 (continued).

Energy average		Assignment	$d\sigma/d\Omega(d,p) \mu b/sr$			$d\sigma/d\Omega(d,t) \mu b/sr$		
(d,p) keV	(d,t) keV		60°	90°	125°	60°	90°	125°
1013			3	4	2			
1049			36	18	8			
1072			16	11	8			
1085			41	21	8			
1101		9/2 5/2 - [512]	7	6	2			
1123			6	3	2			
1145			20	13	6			
1172			29	13	8			
1233 ¹			34	22	10			
1245 ¹			10	7	3			
1296 ²			112	68	29			
1328			11	7	3			
1346			14	19	3			
1379			77	69	24			
1420			89	56	18			
1452			94	47	23			
1484			59	33	19			
1505			37	15	10			
1524			23	6	7			
1569		3/2 1/2 - [510]	112	58	28			
1602			51	29	16			
1632		5/2 1/2 - [510]	32	17	7			
1653*			117	54	30			
1682			38	18	7			
1701		7/2 1/2 - [510]	55	31	20			
1797			46	19	12			
1836			45	21	15			
1978			39	22	15			
2003			71	39	19			
2157			48	27	14			

¹ Not clearly resolved.² Probably double.* Several unresolved (d,p) groups from here and up.

spectra. The resulting level schemes for the six nuclei investigated are presented in Figs. 12-17 whereas Fig. 11 summarizes the energies at which the main components of the single-particle levels have been observed. The

TABLE 3. Levels populated in ^{159}Dy .

Energy average		Assignment	$d\sigma/d\Omega(d,p) \mu\text{b/sr}$			$d\sigma/d\Omega(d,t) \mu\text{b/sr}$		
(d,p) keV	(d,t) keV		60°	90°	125°	60°	90°	125°
0	0	3/2 3/2 - [521]	100	39	12	113	91	52
136	137	7/2 3/2 - [521]	146	105	38	132	132	82
176		5/2 5/2 + [642]	4	1.5	3			
206		7/2 5/2 + [642]	10	2	1			
238	239	9/3 3/2 - [521], 9/2 +	70	47	21	59	68	36
309	309	5/2 5/2 - [523]	32	20	9	11	13	7
	352	11/2 11/2 - [505]				15	50	44
362	365	13/2 +, 11/2 3/2 - [521]	51	54	48	18	65	37
394	395	7/2 5/2 - [523]	115	71	30	24	31	21
416	418	3/2 3/2 + [402] (+ 3/2 + [651])	61	43	15	198	290	153
470	471		2	2	2	5		13
504	506	9/2 5/2 - [523]	21	17	9	3	4	7
533	534	1/2 1/2 - [521]	258	140	45	45	36	11
	549	3/2 3/2 + [651] (+ 3/2 + [402])				66	83	62
560	564	1/2 1/2 + [400]	143	68	29	294	399	278
586		3/2 1/2 - [521]	32	19	8			
	607					12	23	11
621		5/2 1/2 - [521]	60	52	16			
	627	3/2 3/2 - [532]				23	13	15
635		(11/2 5/2 - [523])	13	10	9			
688	690	5/2 3/2 - [532]	16	12	5	41	55	37
744	749	7/2 1/2 - [521], 3/2 1/2 - [530]	165	120	45	70	92	28
772	774	7/2 3/2 - [532], 5/2 1/2 - [530]	19	13	3	21	26	6
798	795		64	36	19	58	63	30
825	828	7/2 1/2 - [530]	9	8	3	32	31	8
854	857		3	3	2	12	8	4
983			17	11	6			
1089		7/2 5/2 - [512]	113	86	35			
1150			22	16	6			
1189		9/2 5/2 - [512]	10	9	5			
1213			8	≤ 11	2			
1283			110	≤ 107	35			
1341			18	13	5			
1391			9	7	6			
1411			26	20	15			
1431			80	41	14			
1473		3/2 1/2 - [510]	132	80	26			
1515			14	14	7			
1535		5/2 1/2 - [510]	27	18	8			

(continued)

TABLE 3 (continued).

Energy average		Assignment	$d\sigma/d\Omega(d,p) \text{ } \mu\text{b/sr}$			$d\sigma/d\Omega(d,t) \text{ } \mu\text{b/sr}$		
(d,p) keV	(d,t) keV		60°	90°	125°	60°	90°	125°
1558		7/2 1/2 - [510]	48	30	13			
1590			35	24	10			
1621			32	21	11			
1643			151	97	31			
1673			26	19	7			
1696			51	34	14			
1727*			52	47	18			
1748			53	33	17			
1786			65	37	15			
1824			54	39	19			
1849			45	32	15			
1891			99	59	21			
1918			43	29	11			
1961			24	18	6			
1989			45	25	24			
2016			63	39	14			

* Several unresolved peaks from here.

identification of the individual quantum states is to a large extent based on a comparison of theoretical and experimental intensities. The data for a number of the more firmly established bands are collected in Tables 9-20.

2.3.1. The 3/2-[521] Orbital

This orbital is characterized by strong 3/2- and 7/2- members of the rotational band. The 9/2- state has approximately 10% of the 7/2- strength, whereas the 5/2- state is very weak and in most cases not observed.

From the angular distributions and the intensity patterns, the ground state in ^{155}Dy , ^{157}Dy , and ^{159}Dy is identified as the 3/2-[521] orbital.

In ^{155}Dy , the 7/2- and the 9/2- states are observed at 134 keV and 223 keV, respectively. The corresponding states in ^{157}Dy are found at 147 keV and 257 keV, and in this nucleus also the 5/2- state is observed at 61 keV with a cross section of approximately 1 $\mu\text{b/sr}$. In ^{159}Dy , the 7/2- state is observed at 137 keV and the 9/2- state at 239 keV. The (d,t) cross section for this level is too large, but this can at least partly be explained by

TABLE 4. Levels populated in ^{161}Dy .

Energy average		Assignment	$d\sigma/d\Omega(d,p) \text{ } \mu\text{b/sr}$			$d\sigma/d\Omega(d,t) \text{ } \mu\text{b/sr}$		
(d,p) keV	(d,t) keV		60°	90°	125°	60°	90°	125°
0	0	5/2 5/2 + [642]	2		3	6	5	2
28	26	5/2 5/2 - [523]	23	20	10	26	23	12
	44	7/2 5/2 + [642]				5	4	2
76	75	3/2 3/2 - [521]	73	29	17	242	183	74
104	101	9/2 + , 7/2 5/2 - [523]	63	49	26	80	84	44
136	132	5/2 3/2 - [521]	9	2	2	9	5	5
197	201	9/2 5/2 - [523]	9	10	7	14	27	18
214	213	7/2 3/2 - [521]	180	124	64	266	217	144
269	268	13/2 +	34	37	30	32	67	48
322	317	9/2 3/2 - [521]	6	2	1	3	6	5
370	368	1/2 1/2 - [521]	258	125	41	98	102	30
421	418	3/2 1/2 - [521]	36	27	7	24	11	7
451	448	5/2 1/2 - [521]	55	48	28	17	35	26
485	486	11/2 11/2 - [505]	7	8	4	27	58	60
512			4	3	2			
553	551	3/2 3/2 + [402] (+ 3/2 + [651])	35	23	14	348	413	214
572	567	7/2 1/2 - [521]	96	66	22	26	19	12
610	608	1/2 1/2 + [400] (+ 1/2 + [660])	58	21	11	278	326	176
634	634	(9/2 1/2 - [521])	24	12	12	8	18	15
682	679	3/2 3/2 + [651] (+ 3/2 + [402])	8	8	9	54	72	56
	717					20	32	13
723			7	9	5			
	730					18	20	11
780	774	1/2 1/2 + [400] (+ 1/2 + [660])	59	27	12	200	260	148
808	801	(11/2 1/2 - [521])	10	9	6	8	14	10
833	827		6	2	3	11	22	11
	850					45	72	49
859	860	3/2 1/2 - [530]	36	39	10	151	148	58
	877	5/2 1/2 - [530]				34	26	16
883		7/2 5/2 - [512]	284	259	115			
928	924		19	38	6	8	7	5
	958	7/2 1/2 - [530]				13	24	17
971	971		8	7	4	11	12	7
995		9/2 5/2 - [512]	10	13	15			
	1007						5	5
	1027					23	27	13
1109			10	10				
	1127					11	19	10
1144	1138		22	18	10	7	12	9

(continued)

TABLE 4 (continued).

Energy average		Assignment	$d\sigma/d\Omega(d,p) \text{ } \mu\text{b/sr}$			$d\sigma/d\Omega(d,t) \text{ } \mu\text{b/sr}$		
(d,p) keV	(d,t) keV		60°	90°	125°	60°	90°	125°
1170	1155					6	5	6
	1182		28	23	21		6	6
	1207					11	14	6
1216			5	6	7			
1260			15	12	7			
	1271					8	8	5
	1290					1.5	6	5
1309		3/2 1/2 - [510]	215	152	68			
1363		5/2 1/2 - [510]	55	43	19			
	1379					11	15	8
1384			35	18	11			
	1416	7/2 7/2 + [404]				29	64	45
1422			55	33	21			
	1436					14	19	10
1446		7/2 1/2 - [510]	43	23	22			
	1460					3.5	6	2
1477			56	27	12			
1516			99	48	16			
1535			86	66	32			
1562			12	6	5			
1594*			31	21	10			
1645			47	21	20			
1712			56	38	19			
1825			70	38	23			
1923			80	51	32			
1946			61	38	25			
1977		3/2 3/2 - [512]	205	124	51			
1996			197	102	54			
2039		5/2 3/2 - [512]	321	172	87			
2113		7/2 3/2 - [512]	85	54	40			

* Several unresolved peaks from here.

the occurrence of the $9/2 \ 5/2 + [642]$ group at the same energy, in accordance with BORGREEN et al.⁴⁾.

The 75 keV level in ^{161}Dy is identified as the band head of the $3/2 - [521]$ band. The $5/2 -$, $7/2 -$, and $9/2 -$ states are then observed at 132 keV, 213 keV, and 317 keV, respectively. Angular distributions and relative cross

TABLE 5. Levels populated in ^{163}Dy .

Energy average		Assignment	$d\sigma/d\Omega(d,p) \text{ } \mu\text{b/sr}$			$d\sigma/d\Omega(d,t) \text{ } \mu\text{b/sr}$		
(d,p) keV	(d,t) keV		60°	90°	125°	60°	90°	125°
0	0	5/2 5/2 - [523]	21	11	6	58	54	25
74	73	7/2 5/2 - [523]	31	18	6	39	43	19
168	167	9/2 5/2 - [523]	17	19	9	32	43	32
	250	5/2 5/2 + [642]				9	4	2
282	281	11/2 5/2 - [523]	4	5	4	7	14	11
	335	9/2 +				91	83	46
350	351	1/2 1/2 - [521]	249	115	42	127	74	29
388		3/2 1/2 - [521]	9	3	1			
(421)	421	3/2 3/2 - [521]	16	8	3	341	221	107
425		5/2 1/2 - [521]	114	57	17			
476	474	5/2 3/2 - [521]	14	8	2	16	14	7
	495	11/2 11/2 - [505]				48	75	67
499		9/2 7/2 + [633]	27	31	24			
517	514	7/2 1/2 - [521], 13/2 +	175	116	53	157	150	84
556	552	7/2 3/2 - [521]	46	28	9	173	152	81
592			9	3	2			
	644	9/2 3/2 - [521]				6	13	13
651			11	8	7			
719	715	13/2 7/2 + [633]	15	20	9	2	8	15
740	736	1/2 1/2 + [660] (+ 1/2 + [400])	16	15	5	123	101	54
	764	11/2 3/2 - [521] (3/2 1/2 + [660])				13	24	27
	780	(5/2 1/2 + [660])				5	10	10
	794					81	55	29
801		7/2 5/2 - [512]	520	306	133			
	820					7	6	2
827			20	12	9			
861	857	3/2 3/2 + [402] (+ 3/2 + [651])	34	21	15	469	526	380
887	883		48	30	16	79	80	48
918	912	9/2 5/2 - [512]	14	9	8	24	28	29
	933					23	23	17
949	945		92	65	29	14	16	12
	989					4	13	20
1058	1057	1/2 1/2 + [400] (+ 1/2 + [660])	83	43	24	556	539	352
1087	1084	(3/2 3/2 + [651] (+ 3/2 + [402]))	6	7	5	40	49	32
1126	1129		15	20	18	50	66	59
1159		(1/2 1/2 - [510])	6	9	10			
1199	1199	3/2 1/2 - [510]	323	180	73	43	44	27
	1252					6	11	6
1262		5/2 1/2 - [510]	99	67	30			

(continued)

TABLE 5 (continued).

Energy average		Assignment	$d\sigma/d\Omega(d,p) \mu b/sr$			$d\sigma/d\Omega(d,t) \mu b/sr$		
(d,p) keV	(d,t) keV		60°	90°	125°	60°	90°	125°
1284	1275	3/2 1/2 - [530]	14	6	6	74	60	30
1342	1295					4		3
	1359	7/2 1/2 - [510]	40	30	18			
	1425	7/2 1/2 - [530]				9	24	14
1448*		(9/2 1/2 - [530])				13	15	15
	1481		24	12	5			
1494	1497		14	4	3	6	5	2
	1526					12	16	10
1533			38	18	11	14	19	10
1549			71	57	30			
	1570					11	11	5
1597			10	9	4			
	1611					8	12	5
1629	1630		26	24	11	20	30	25
1663			22	11	3			
1696	1689		40	20	7	12	9	10
1713	1706		35	19	8	22	38	37
1734			38	31	15			
	1751					31	31	23
1795		3/2 3/2 - [512]	308	169	57			
	1806					3	5	3
1817			114	62	18			
	1840	7/2 7/2 + [404]				35	50	43
1856		5/2 3/2 - [512]	432	232	116			
1936		7/2 3/2 - [512]	169	85	40			
1957			170	79				
1988			258	109	42			
2012			95	42	30			
2067			54	35	10			
2087			37		8			
2114			81		18			
2169			104	32	15			
2317			120	81	38			
2351			72	37	17			

* Several unresolved peaks from here.

TABLE 6. Levels populated in ^{165}Dy .

Energy average (d,p) keV	Assignment	$d\delta/d\Omega(d,p) \mu\text{b/sr}$		
		60°	90°	125°
0	7/2 7/2 + [633]	2		
84	9/2 7/2 + [633]	22	14	4
109	1/2 1/2 - [521]	295	164	59
158	3/2 1/2 - [521]	7	15	1
182	5/2 1/2 - [521], 5/2 5/2 - [512]	76	66	22
262	7/2 5/2 - [512]	250	218	110
298	7/2 1/2 - [521]	117	99	54
308	13/2 7/2 + [633]	27	44	23
336	9/2 1/2 - [521]	8	7	5
361	9/2 5/2 - [512]	11	6	5
480	(11/2 5/2 - [521])	8	6	4
518	11/2 1/2 - [521]	8	5	4
535		5	5	2
575		36	12	3
606	3/2 1/2 - [510] + 5/2 - [512] γ -vib	246	143	50
629		39	24	4
658	5/2 1/2 - [510] + 5/2 - [512] γ -vib	48	30	
705		98	67	35
737	7/2 1/2 - [510] + 5/2 - [512] γ -vib	7	10	6
803		4		3
919			4	6
1052		8	7	3
1103		22	10	4
1139		11	8	8
1162		108	85	43
1258	3/2 3/2 - [512]	130	69	25
1283		15	7	5
1312	5/2 3/2 - [512]	156	103	49
1340		172	81	25
1384		272	121	67
1402	7/2 3/2 - [512]	108	53	18
1447		54	16	15
1478		14	9	13
1503		239	120	48
1561		368	174	82
1596		268	172	80
1625		27	11	5
1649		113	71	39
1699		91	62	28
1723		41	42	19

(continued)

TABLE 6 (continued).

Energy average (<i>d,p</i>) keV	Assignment	$d\sigma/d\Omega(d,p) \text{ } \mu\text{b/sr}$		
		60°	90°	125°
1751		85	59	22
1780		17	12	6
1805		9	8	5
1833		91	64	37
1861		56	41	17
1891		44	20	19
1916		23	18	18
1947		45	34	24
1970		28	22	13
2000		9	9	11
2027*		25	20	10
2097			35	17
2121			16	6
2178			78	37
2208			25	14
2294			35	33
2320			74	33
2371			46	23
2432			62	27
2445			46	26
2459			118	50
2495			98	45

* Several unresolved levels from 2027 keV to 2495 keV.

sections agree well with this assignment, which is also in agreement with the ^{161}Tb measurements⁵⁾.

The $3/2 - [521]$ band in ^{163}Dy shown in Fig. 16 is in agreement with that proposed by SCHULT et al.⁶⁾. The observed states fit well into the intensity pattern for the different members of the rotational band, although the $7/2 -$ state in ^{163}Dy is weak compared to the same state in ^{161}Dy .

The ^{165}Dy nucleus can be reached by the (*d,p*) reaction only. The $3/2 - [521]$ state in ^{165}Dy is a hole excitation and only a small cross section is expected. A band comprising the levels⁷⁻¹⁰⁾ 573.6 keV ($3/2 -$), 628.8 keV ($5/2 -$), and 705.9 keV ($7/2 -$) has been associated with the $3/2 - [521]$ band or with a γ -vibration built on the $1/2 - [521]$ state. Neither of these suggestions does directly explain the rather strong (*d,p*) groups observed (cf. Table 6).

The $3/2 - [521]$ orbital is the ground state in the three successive nuclei ^{155}Dy , ^{157}Dy , and ^{159}Dy . A similar persistence is found in the isobars ^{155}Gd , ^{157}Gd , and ^{159}Gd and might be explained by changes in deformation with increasing neutron number.

It should also be noted that, according to the Nilsson scheme, one would expect the $11/2 - [505]$ state to be the ground state in nuclei with $N = 91$ for a deformation $\delta \sim 0.3$. SOLOVIEV and VOGEL¹³⁾ have made calculations of states close to one-quasiparticle states, taking into account the interaction of quasiparticles with phonons. Their calculations show that the $K = 11/2$ and $9/2$ states are purer one-quasiparticle states (95–99%) than the $K = 1/2$ and $3/2$ states (90–97%). As a consequence, the energies of the low K states are lowered more than the energies of the high K states. The latter are therefore not likely to be ground states if there are near-lying low K orbitals in the Nilsson scheme.

2.3.2. The $1/2 + [660]$, $3/2 + [651]$, and $5/2 + [642]$ Orbitals

The three near-lying orbitals $1/2 + [660]$, $3/2 + [651]$, and $5/2 + [642]$, and partly also $7/2 + [633]$, are expected to give rise to low-lying states in the dysprosium nuclei. These orbitals originate in the $i_{13/2}$ shell-model state and the wave functions of the deformed states have preserved their $i_{13/2}$ character insofar as the coefficients $C_{6,13/2}$ are all close to unity. In addition, there are small admixtures of the $g_{9/2}$ shell-model state. Consequently, only the $9/2 +$ and $13/2 +$ states of the rotational bands have observable cross sections in the (d,p) and (d,t) reactions.

The localization of states belonging to the orbitals discussed above is complicated by coupling effects of Coriolis and $\Delta N = 2$ type, which quite generally affect the even parity states in the deformed nuclei in this region^{14, 15)}. The above-mentioned orbitals are coupled by the Coriolis force with matrix elements which, for the $13/2 +$ states, can be as large as 400 keV. As the expected energy separation of the bands is often much less, the wave functions become completely intermixed. This results in strongly enhanced transfer cross sections for the lowest $9/2 +$ state and the lowest $13/2 +$ state and almost vanishing cross sections for the higher states. Therefore, essentially only one $9/2 +$ and one $13/2 +$ state are observable.

The rotational band structures are greatly affected by the Coriolis coupling, the general effect being a compression of the lowest band and an expansion of the higher bands.

In ^{155}Dy , no $9/2 +$ or $13/2 +$ states have been observed with certainty in this work. In ^{157}Dy , the peak at 161 keV has an angular distribution

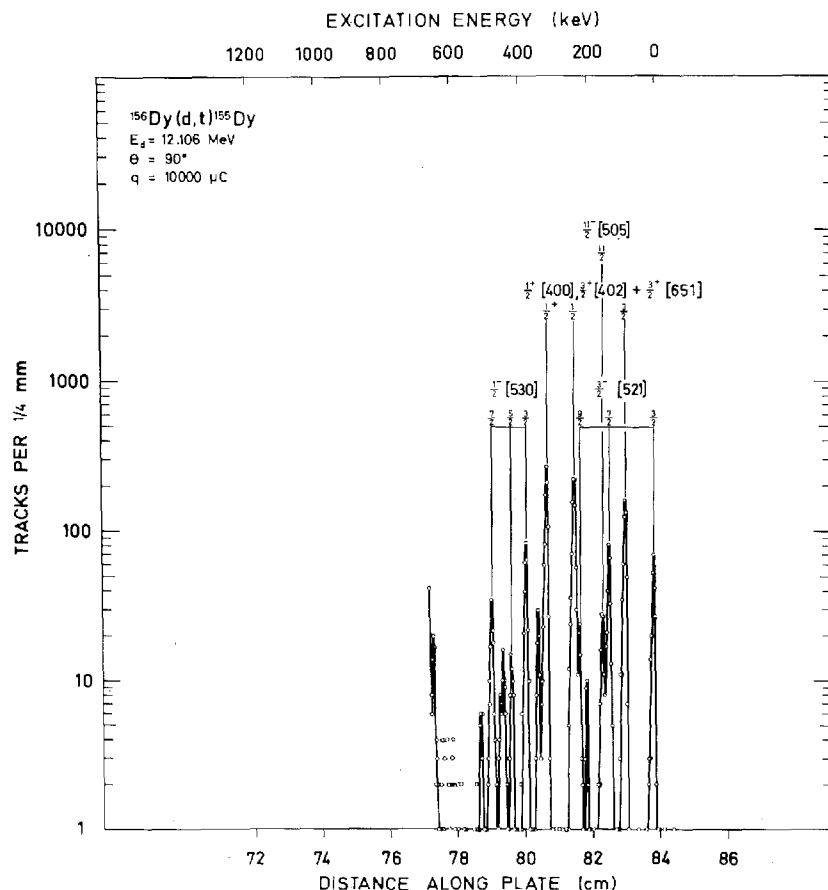


Fig. 1. Triton spectrum for the reaction $^{156}\text{Dy}(d,t)^{155}\text{Dy}$, $\theta = 90^\circ$.

which is consistent with $l = 4$ and has been assigned to the $9/2+$ state. The peak at 350 keV is tentatively assigned to the $13/2+$ state although it is weaker than expected.

In ^{159}Dy , the energy of the peak at 239 keV corresponds to the $9/2$ member of the ground-state rotational band. The cross section is, however, more than twice as strong as expected from the intensity pattern of the $3/2 - [521]$ orbital, and it is assumed that the $9/2+$ state coincides with the $9/2$ $3/2 - [521]$ state. The observed cross section is in reasonable agreement with the expected sum of the two states. The 365 keV group in ^{159}Dy is also double and contains the $11/2$ $3/2 - [521]$ state and the $13/2+$ state. The cross section of the $11/2-$ state, as estimated from the $3/2$ $3/2 - [521]$ cross section, should

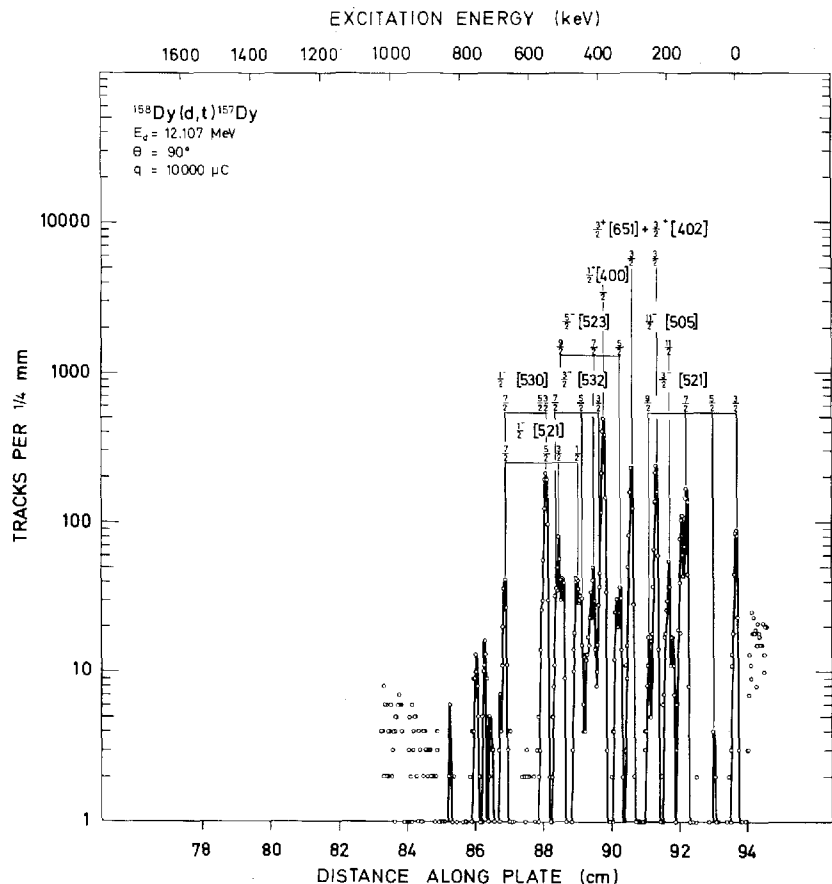


Fig. 2. Triton spectrum for the reaction $^{158}\text{Dy}(d,t)^{157}\text{Dy}$, $\theta = 90^\circ$.

not exceed $8 \mu\text{b/sr}$, so the main part of the cross sections is due to the $13/2+$ state. The angular distributions confirm the assignment. The weak levels at 176 keV and 206 keV are tentatively assigned to the $5/2+$ and $7/2+$ members of the rotational band. The band is found to be severely distorted, but the lower spin states correspond mostly to the $5/2+ [642]$ orbital.

In ^{161}Dy , the $5/2+ [642]$ orbital forms the ground state, and a rotational band up to and including $13/2+$ is observed in the (d,t) spectra with the exception of the $11/2+$ state. The $9/2+$ level at 101 keV coincides with the $7/2 \ 5/2- [523]$ level, but from comparison with the $7/2 \ 5/2- [523]$ state in the neighbouring nuclei, the $9/2 \ 5/2+ [642]$ state can be estimated to contribute with approximately 50% of the observed cross section. The ground-

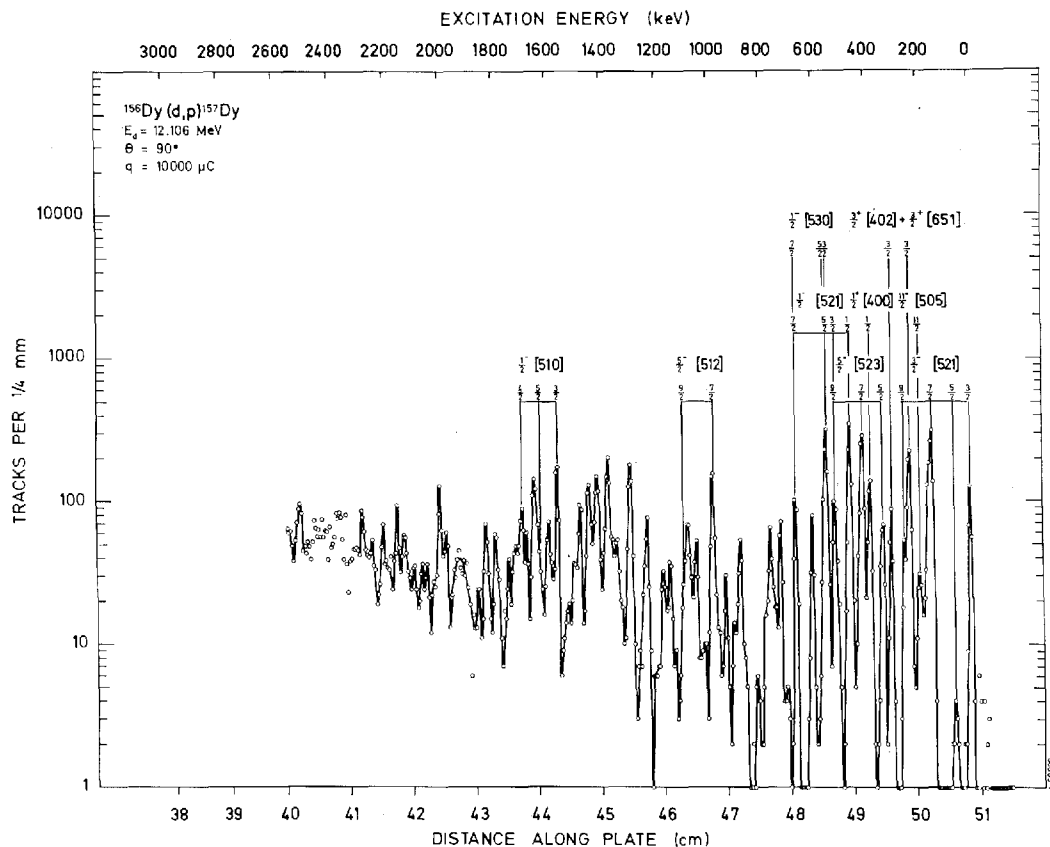


Fig. 3. Proton spectrum for the reaction $^{156}\text{Dy}(d,p)^{157}\text{Dy}$, $\theta = 90^\circ$.

state rotational band has a rotational parameter $A = 6.3 \text{ keV}$. The compression of the rotational band can be ascribed mostly to the Coriolis coupling to the two near-lying orbitals $3/2 + [651]$ and $7/2 + [633]$. The $7/2 + [633]$ orbital is expected as a particle state at approximately 400 keV of excitation energy and the $3/2 + [651]$ orbital is a hole state at approximately 700 keV.

In ^{163}Dy , the $5/2 + [642]$ state is previously known as a hole state. In the present work, the $5/2 +$ state is observed as a weakly populated level at 250 keV. The $9/2 +$ state observed at 335 keV has an angular distribution consistent with $l = 4$. The $13/2 +$ state is expected to have approximately the same strength as the $9/2 +$ state in ^{163}Dy , and it is tentatively assumed that it coincides with the $7/2 \ 1/2 - [521]$ state at 514 keV. If we compare the (d,p) and the (d,t) cross sections of the different members of the rotational

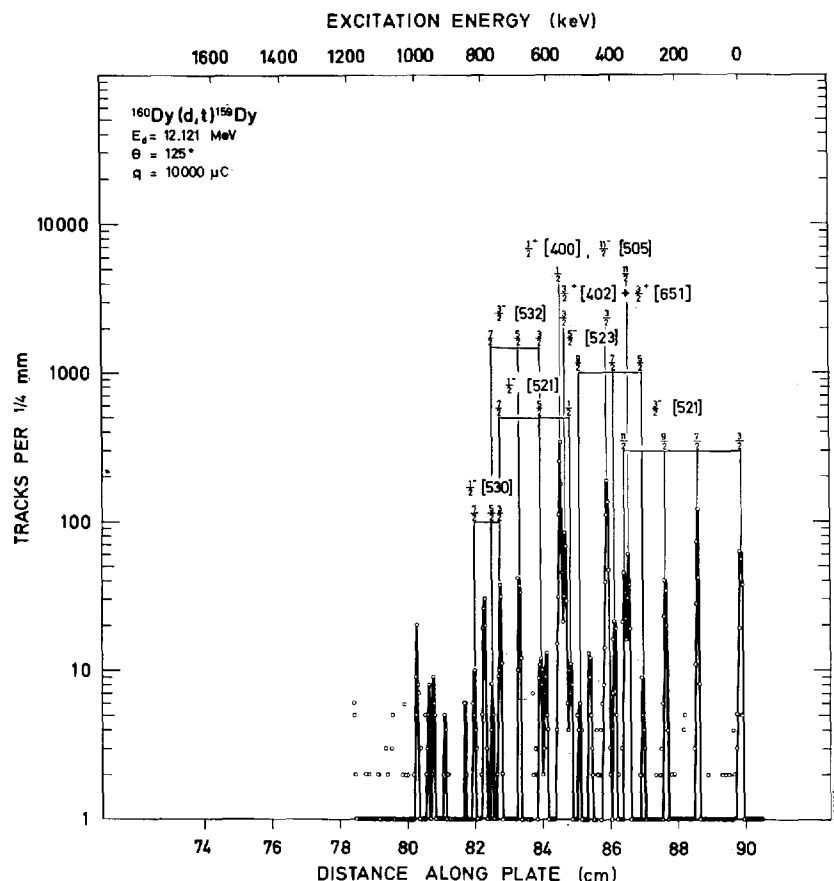


Fig. 4. Triton spectrum for the reaction $^{160}\text{Dy}(d,t)^{159}\text{Dy}$, $\theta = 125^\circ$.

band which is built on the $1/2 - [521]$ orbital, the (d,t) cross section is found to be 45% of the (d,p) cross section at 90° for the $1/2 \ 1/2 - [521]$ state, as compared to the peak at 514 keV where the (d,t) cross section is 105% of the (d,p) cross section. It is therefore proposed that the $13/2 +$ group is contained in the group at 514 keV.

Table 10 collects the information on $9/2 +$ and $13/2 +$ states which, according to the discussion above, are ascribed to the lowest of the coupled $N = 6$ states. Some of the assignments are based on insufficient experimental evidence and must therefore be regarded with some caution. The average cross section for the $9/2 +$ states is almost 1.6 times larger than expected for a pure state. The corresponding ratio for the $13/2 +$ states is 2.4. Both

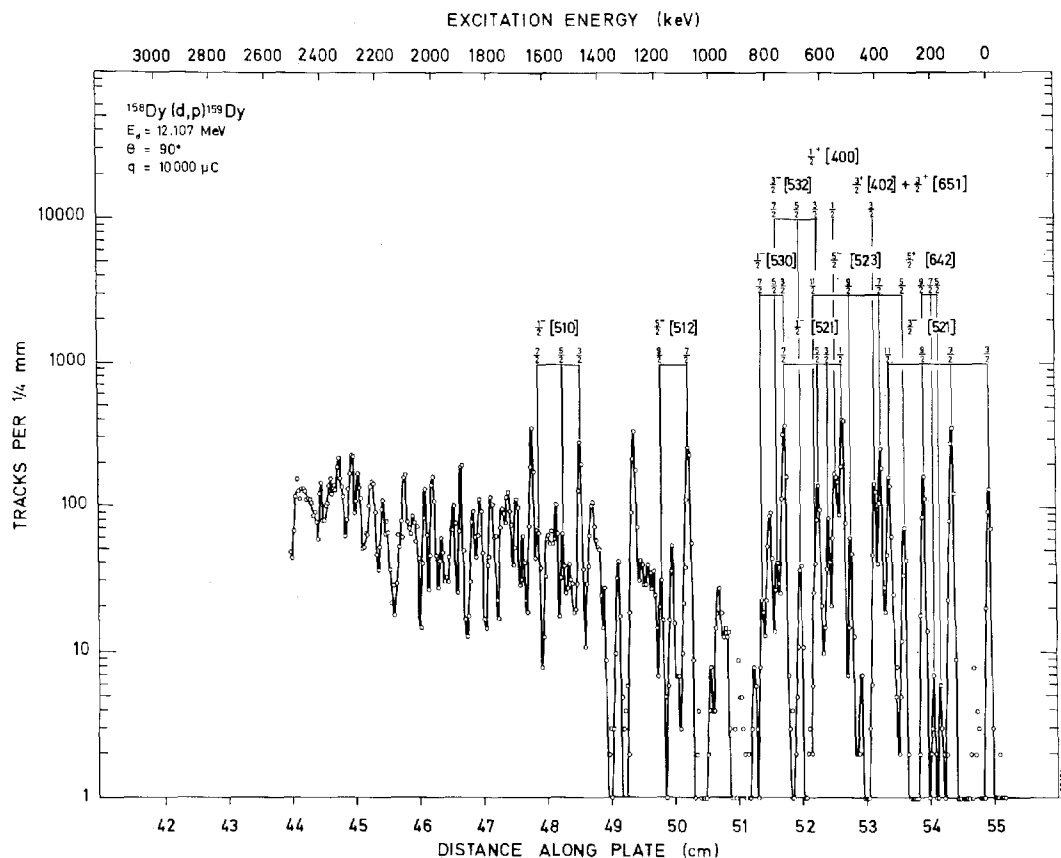


Fig. 5. Proton spectrum for the reaction $^{158}\text{Dy}(d,p)^{159}\text{Dy}$, $\theta = 90^\circ$.

values show the influence of the Coriolis coupling effects on the cross section of the high angular momentum states.

Whereas the Coriolis coupling mostly affects the high spin states, the $\Delta N = 2$ coupling is of importance for the low spin states. The dysprosium nuclei present the most complete example observed so far of the coupling of the crossing states $3/2 + [402]$ and $3/2 + [651]$. In addition, some effects of the crossing of the $1/2 + [400]$ and $1/2 + [660]$ can be identified. The $\Delta N = 2$ coupling of the strongly populated $3/2 + [402]$ state to the $3/2 + [651]$ state gives rise to a splitting of the $3/2 +$ strength which relatively easily is located in the spectra. The experimental evidence is discussed below.

In ^{155}Dy , the level at 86 keV has an angular distribution of the (d,t)

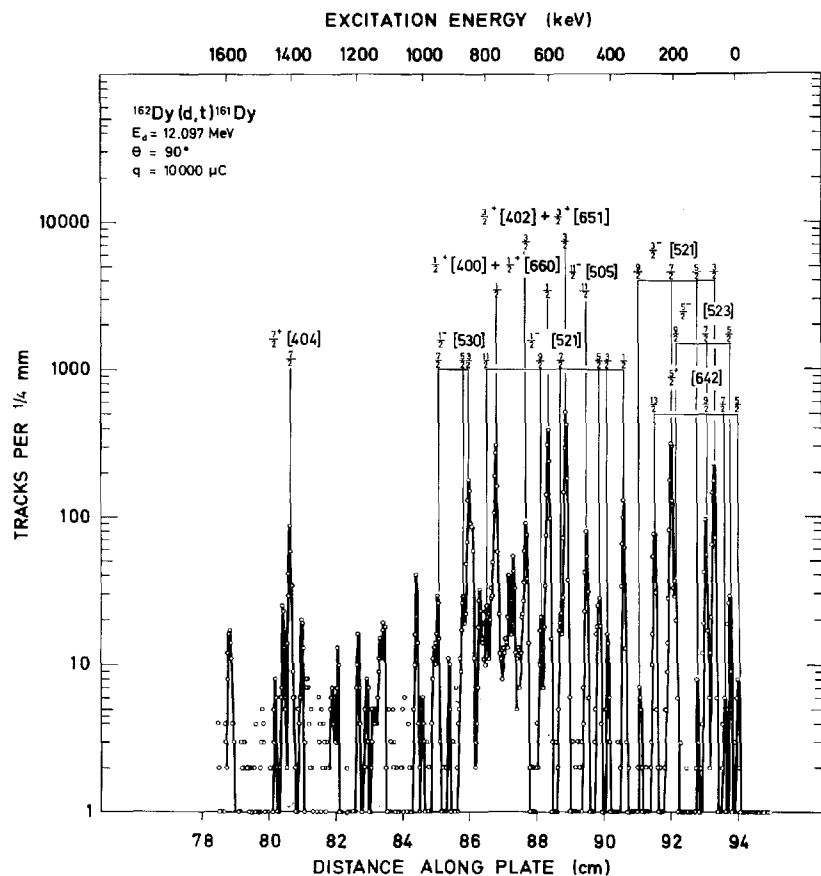


Fig. 6. Triton spectrum for the reaction $^{162}\text{Dy}(d,t)^{161}\text{Dy}$, $\theta = 90^\circ$.

cross section which is consistent with $l = 2$, and is also similar to the (d,t) angular distribution of the strong group at 239 keV which represents most of the $3/2 \ 3/2 + [402]$ strength. The 86 keV level therefore is assigned to the $3/2 + [651]$ state with admixture of the $3/2 \ 3/2 + [402]$ state.

In ^{157}Dy , the levels at 235 keV and 307 keV are about equally populated and have very similar angular distributions which are consistent with $l = 2$. The two levels are therefore assigned to the coupling orbitals $3/2 + [651]$ and $3/2 + [402]$.

In ^{159}Dy , the 549 keV level has an $l = 2$ angular distribution and is assigned to the $3/2 + [651]$ ($+ 3/2 + [402]$) state. The coupling is obviously weaker in this case.

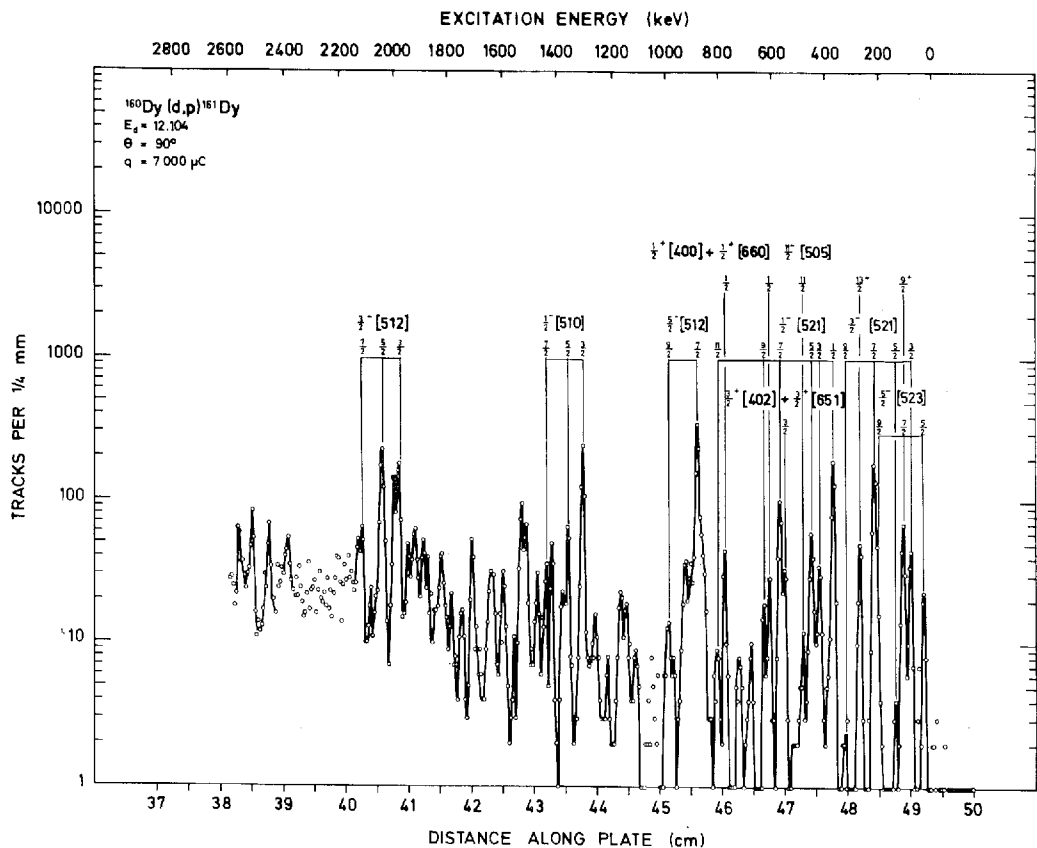


Fig. 7. Proton spectrum for the reaction $^{160}\text{Dy}(d,p)^{161}\text{Dy}$, $\theta = 90^\circ$.

In ^{161}Dy , the level at 679 keV has an $l = 2$ angular distribution and a strength which strongly suggests a $3/2 + [651]$ ($+ 3/2 + [402]$) assignment.

Finally, in ^{163}Dy , the level at 1084 keV is suggested for the same assignment, but the experimental evidence is meager.

In analogy to the case discussed above, the $1/2 + [660]$ orbital couples to the $1/2 + [400]$ orbital, but evidence for this coupling has, however, not been observed in the three lightest nuclei, ^{155}Dy , ^{157}Dy , and ^{159}Dy , investigated in this work.

In ^{161}Dy , the angular distributions of the (d,p) as well as the (d,t) cross sections for the 608 keV level are very similar to those for the 774 keV group. Both of these groups have $l = 0$ angular distributions and are there-

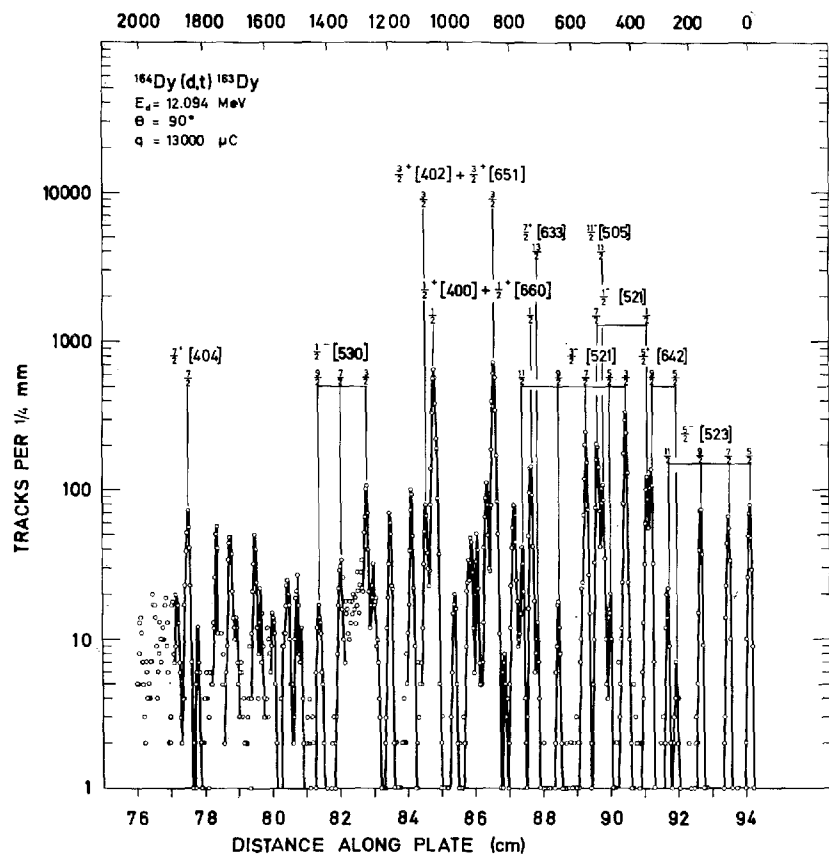


Fig. 8. Triton spectrum for the reaction $^{164}\text{Dy}(d,t)^{163}\text{Dy}$, $\theta = 90^\circ$.

fore assigned to the $1/2 + [660] + 1/2 + [400]$ state. Each group represents approximately 50% of the $1/2 + [400]$ strength.

In ^{163}Dy , the group at 736 keV is ascribed to the $1/2 + [660]$ ($+ 1/2 + [400]$) state from the angular distribution of the (d,t) cross section. The 736 keV level is previously proposed⁶⁾ to contain also the gamma vibration built on the $5/2 + [642]$ state and the suggested $3/2 +$ and $5/2 +$ members of the rotational band are observed in the (d,t) spectrum. The corresponding low decoupling parameter, $a = 0.5$, seems hard to reconcile with the large fraction ($\sim 80\%$) of the $1/2 + [660]$ state indicated by the fraction present of the $1/2 + [400]$ state.

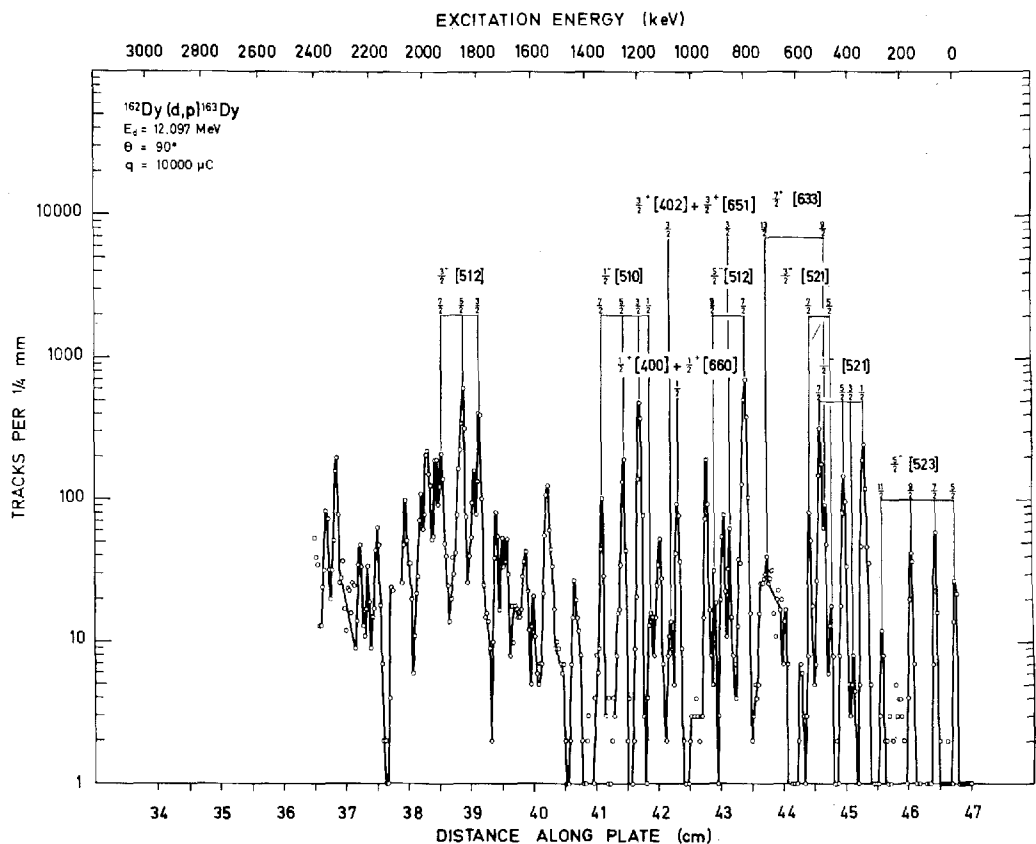


Fig. 9. Proton spectrum for the reaction $^{162}\text{Dy}(d,p)^{163}\text{Dy}$, $\theta = 90^\circ$.

2.3.3. The $3/2 + [402]$ Orbital

This orbital is expected to give rise to strong groups in the (d,t) spectra. As mentioned in sect. 2.3.2, a strong $\Delta N = 2$ coupling to the $3/2 + [651]$ orbital is observed in all of the Dy nuclei investigated, except ^{165}Dy .

The angular distributions of the (d,t) cross sections are very similar for the $3/2 + [402]$ and $1/2 + [400]$ states and it is impossible on this basis to distinguish one from the other. The angular distributions of the (d,p) cross sections are, however, different for the two orbitals, which allows an identification since the spin and parity of one of the states in question are determined in ^{163}Dy (860 keV, $3/2 +$) and in ^{161}Dy (551 keV, $3/2 +$) from other experiments^{6, 18}.

In ^{155}Dy , the 239 keV level is ascribed to the $3/2 + [402]$ orbital from

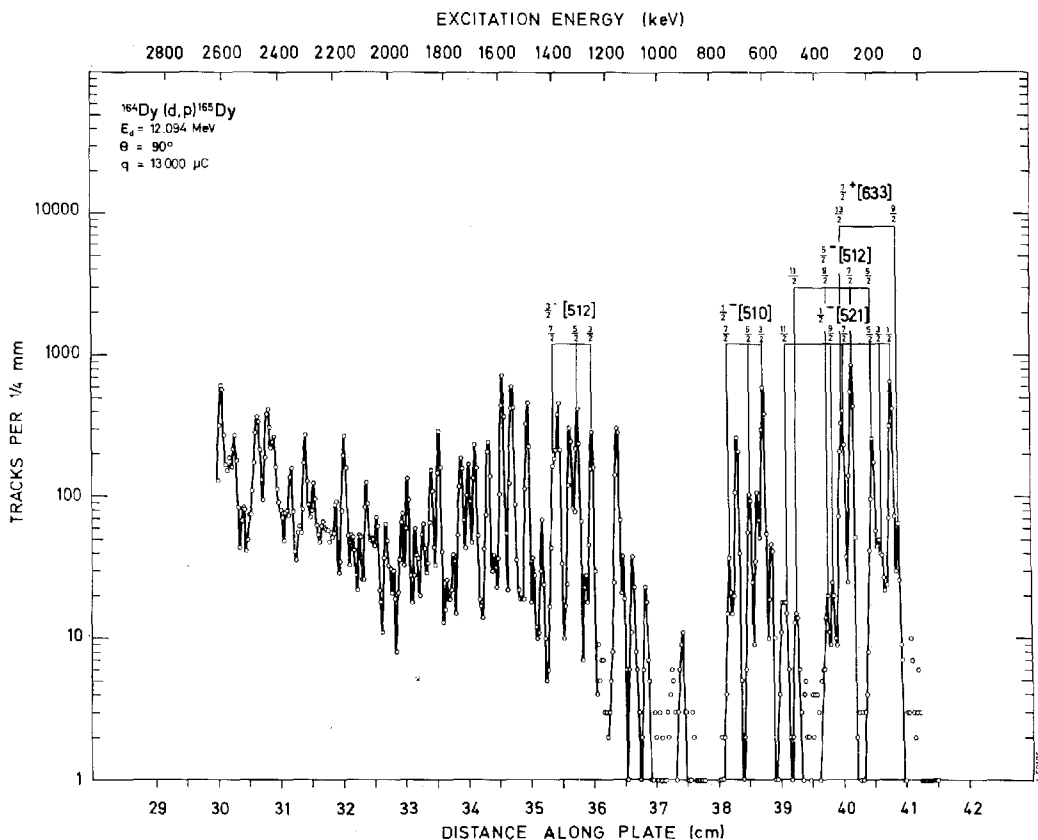


Fig. 10. Proton spectrum for the reaction $^{164}\text{Dy}(d,p)^{165}\text{Dy}$, $\theta = 90^\circ$.

the angular distribution and from energy systematics. The strength is split between this level and the 86 keV level.

In ^{157}Dy , the $3/2 + [402] + 3/2 + [651]$ level is observed at 307 keV, and the strength is here almost equally split between this level and the 235 keV level. The levels are identified by the angular distribution of the (d,p) cross sections.

In ^{159}Dy , the 418 keV level is identified as the $3/2 + [402]$ ($+ 3/2 + [651]$) state from the angular distribution of the (d,p) cross section. The main part of the strength is observed in this level, and the remainder is found in the 549 keV level.

The $\Delta N = 2$ coupling is still weaker in ^{161}Dy , where most of the $3/2 + [402]$ state strength is observed at 551 keV, and in ^{163}Dy where the strength is

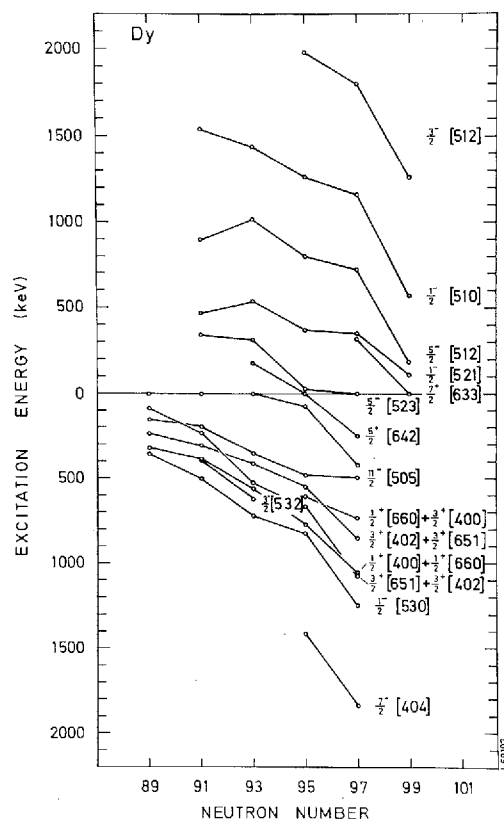


Fig. 11. Energies of the band heads for Nilsson states observed. Points at negative energies indicate hole states.

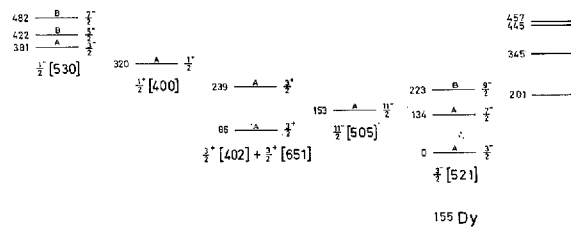


Fig. 12. Level scheme for ^{155}Dy .

TABLE 7. Q -values and neutron separation energies for Dy nuclei.

Mass A	$Q(d,t)$ $A \rightarrow A-1$ keV	$Q(d,p)$ $A-1 \rightarrow A$ keV	$S_n(d,t)$ keV	$S_n(d,p)$ keV	S_n from mass tables ¹ keV
156	-3184 ± 10		9442 ± 10		9890 ± 1010
157		4753 ± 10		6978 ± 10	6830 ± 1010
158	-2804 ± 10		9062 ± 10		8840 ± 1000
159		4600 ± 10		6825 ± 10	6851 ± 34
160	-2323 ± 10		8581 ± 10		8590 ± 30
161	-205 ± 10	4237 ± 10	6463 ± 10	6462 ± 10	6448 ± 12
162	-1944 ± 10	5981 ± 10	8202 ± 10	8206 ± 10	8204 ± 9
163	-27 ± 10	4045 ± 10	6285 ± 10	6270 ± 10	6253 ± 5
164	-1407 ± 10	5441 ± 10	7665 ± 10	7666 ± 10	7656.8 ± 4
165		3496 ± 10		5721 ± 10	5635 ± 10

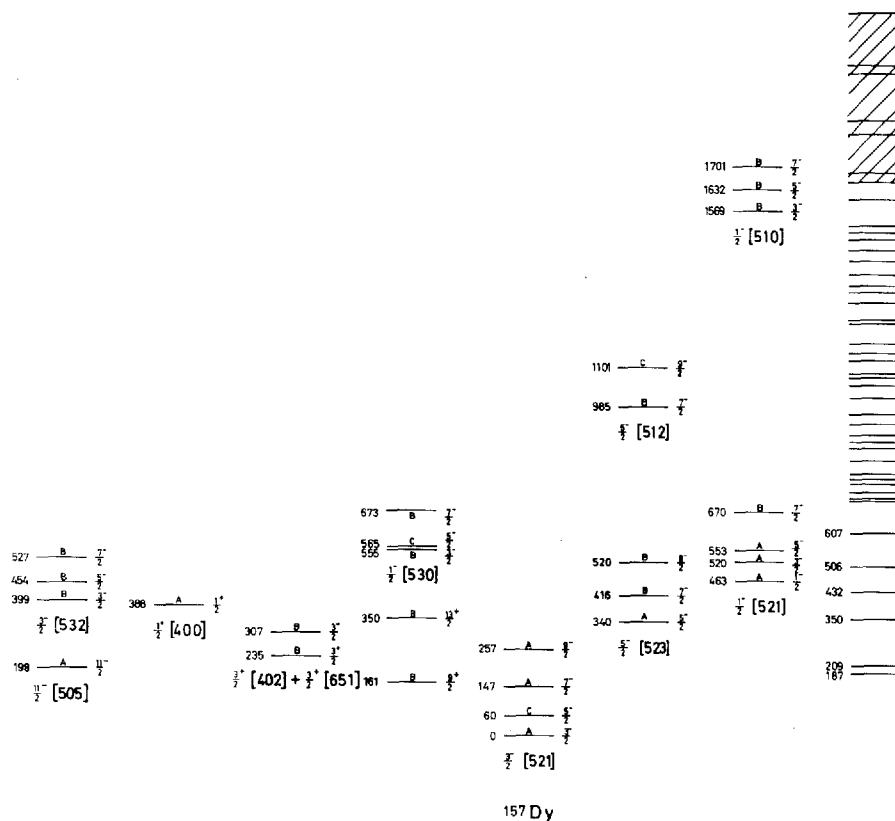
¹ I. H. E. MATTAUCH et al., Nucl. Phys. 67 (1965) 32.TABLE 8. Unperturbed energy difference ΔH and $\Delta N = 2$ matrix element V for the $3/2 + [402] + 3/2 + [651]$ and the $1/2 + [400] + 1/2 + [660]$ orbitals in different Dy nuclei.

A	$3/2 + [402] + 3/2 + [651]$		$1/2 + [400] + 1/2 + [660]$	
	ΔH (keV)	V (keV)	ΔH (keV)	V (keV)
155	53	72		
157	1.3	36		
159	-67	56		
161	-86	47	-2.5	83
163	-183	68	240	107

TABLE 9. (d,t) population of the $3/2 - [521]$ band*.

Spin	$d\sigma/d\Omega, \theta = 90^\circ, Q = -2 \text{ MeV}$						Relative value of C_{Ji}^2					
	Theory	155	157	159	161	163	Theory	155	157	159	161	163
3/2	167	123	106	114	185	197	0.10	0.08	0.10	0.12	0.18	0.22
5/2			1		5	13			~ 0		0.01	0.04
7/2	297	174	216	173	242	148	0.53	0.32	0.53	0.51	0.68	0.47
9/2	22	52	23	~ 20	7	13	0.26	0.60	0.37	0.37	0.13	0.27
11/2	10						0.11					

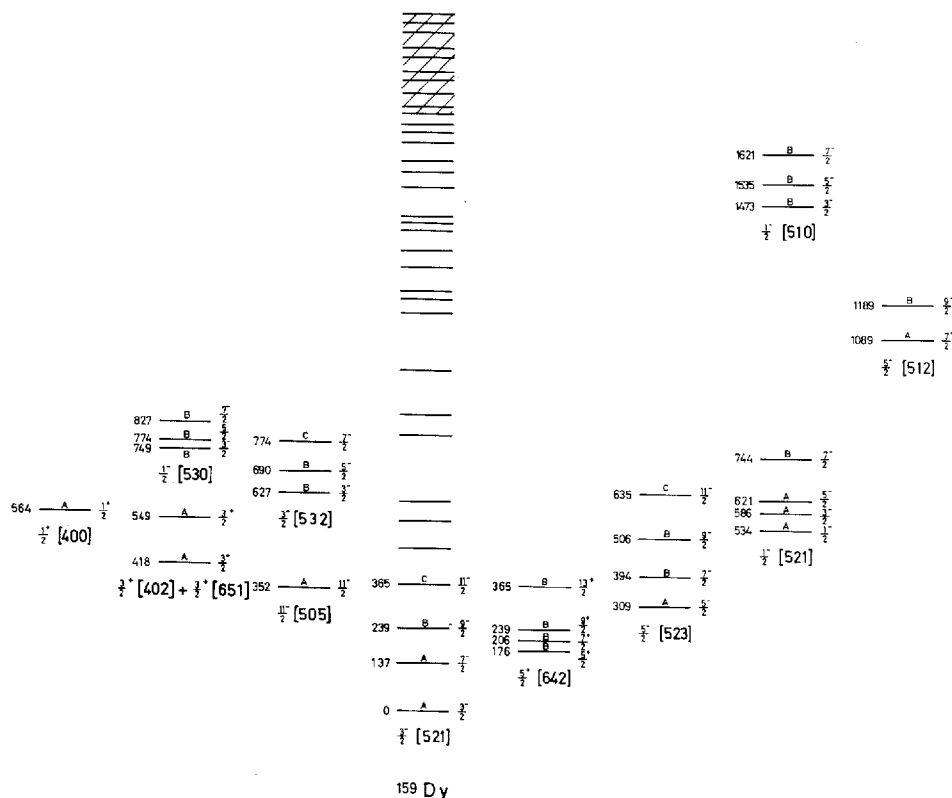
* All cross sections in Tables 9-20 are given in $\mu\text{b/sr}$.

Fig. 13. Level scheme for ^{157}Dy .

observed in the 860 keV level. The splitting of the (d,t) cross sections on the $3/2 + [402] + 3/2 + [651]$ states is shown in Fig. 18, whereas the summed cross section is illustrated in Fig. 19.

The $\Delta N = 2$ coupling of the $1/2 + [660]$ and $1/2 + [400]$ states in ^{159}Gd has earlier been considered in some detail¹⁶⁾. A derivation of the coupling matrix element V between the $3/2 + [651]$ and $3/2 + [402]$ states is now possible for all the Dy nuclei on the basis of the two components of the $3/2 + [402]$ state identified in each nucleus. If α is the $N = 4$ amplitude in the upper state and β the $N = 4$ amplitude in the lower state, one has for V and the uncoupled energy separation ΔH

$$|V| = \frac{|\alpha/\beta|}{(\alpha/\beta)^2 + 1} \Delta E \quad (1)$$



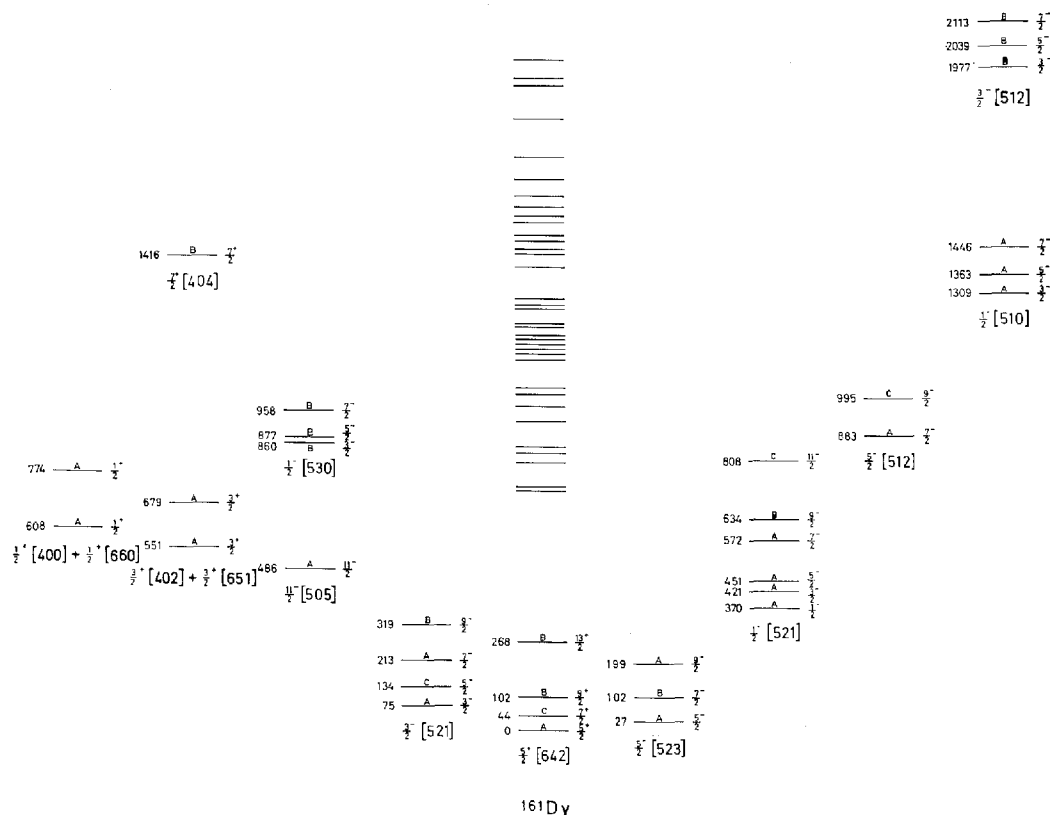


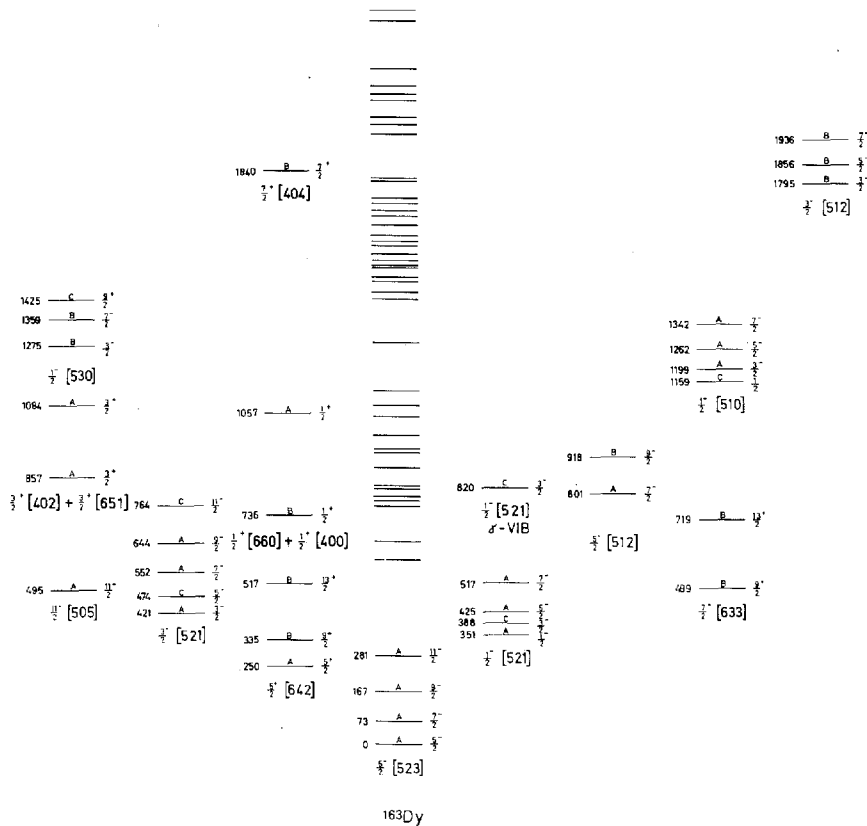
Fig. 15. Level scheme for ^{161}Dy .

bered that the influence of other couplings has been neglected. An estimate of the Coriolis coupling to the $1/2 + [660]$ band shows that the values of V and ΔH might be affected by $\sim 20\%$.

2.3.4. The $1/2 + [400]$ Orbital

From the strength of the cross section, the (d,t) angular distribution and from energy systematics the 320 keV level in ^{155}Dy are ascribed to the $1/2 + [400]$ orbital. Similarly, the levels at 388 keV in ^{157}Dy and at 564 keV in ^{159}Dy are assigned to this orbital on the basis of the (d,p) and (d,t) angular distributions and from the strength of the (d,t) cross section.

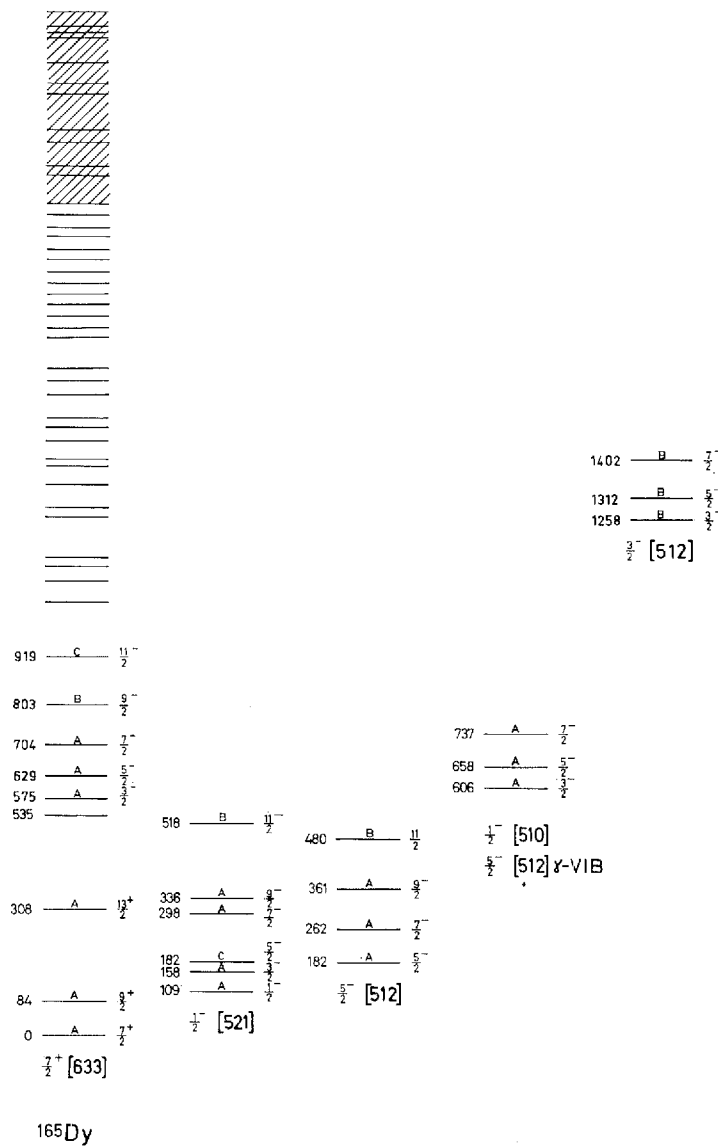
In ^{161}Dy , the $1/2 + [400]$ strength is almost equally divided between the levels at 608 keV and 774 keV. These levels have very similar angular

Fig. 16. Level scheme for ^{163}Dy .

distributions for the (d,p) as well as for the (d,t) reactions, and the angular distributions are typical for $l = 0$.

The strong peak at 1057 keV in ^{163}Dy is ascribed to the $1/2 + [400]$ orbital from the angular distributions of the (d,p) and (d,t) cross sections. The $1/2 + [660]$ state is previously proposed⁶⁾ to be at 736 keV. The strength of the 736 keV group suggests that, due to the $\Delta N = 2$ coupling, it contains part of the $1/2 + [400]$ strength.

The matrix element V and the unperturbed energy separation ΔH have also been derived for the coupling of the $1/2 + [660]$ and the $1/2 + [400]$ states in ^{161}Dy and ^{163}Dy . The results are given in Table 8.

Fig. 17. Level scheme for ^{165}Dy .

2.3.5. The $11/2-[505]$ Orbital

The $11/2-[505]$ orbital is found in all Dy nuclei investigated, except ^{165}Dy which could be reached by the (d,p) reaction only. The identification is based mostly on the characteristic angular distributions of the (d,t) cross sections.

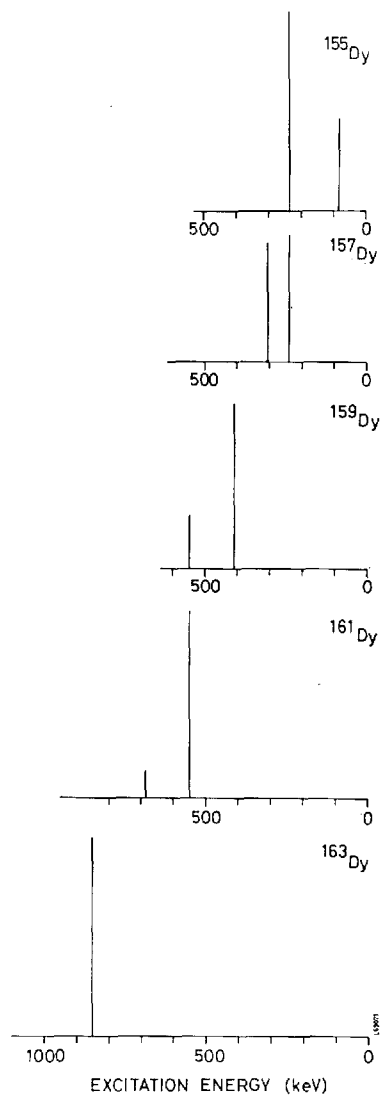


Fig. 18. Relative strength of the $\Delta N = 2$ coupled $3/2 + [651]$ and $3/2 + [402]$ orbitals for different dysprosium nuclei.

In ^{155}Dy , the $11/2 - [505]$ orbital is observed at 153 keV and in ^{157}Dy it is observed at 198 keV.

In ^{159}Dy , the 352 keV level is ascribed to the $11/2 - [505]$ orbital, which is in agreement with data from the $^{160}\text{Dy}(^3\text{He}, \alpha)^{159}\text{Dy}$ reaction¹⁷⁾. In this nucleus, the $11/2 - [505]$ state is observed as an isomeric state⁴⁾.

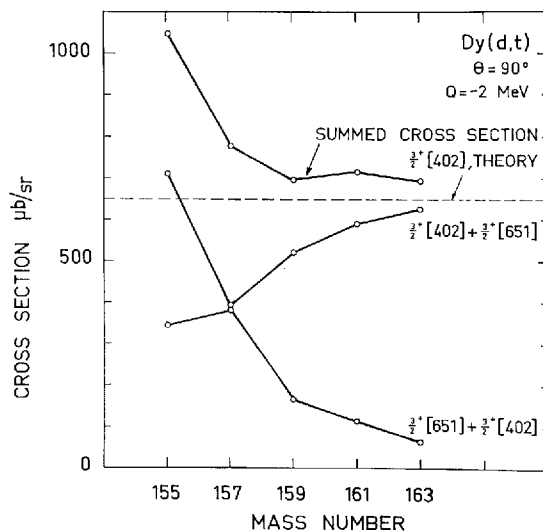


Fig. 19. Summed (d,t) cross sections for the $\Delta N = 2$ coupled $3/2 + [651]$ and $3/2 + [402]$ orbitals.

From the strength and from the angular distribution of the (d,t) cross section, the level at 486 keV in ^{161}Dy and the level at 495 keV in ^{163}Dy are assigned to the $11/2 - [505]$ orbitals in these nuclei.

2.3.6. The $3/2 - [532]$ Orbital

This orbital is observed in ^{157}Dy and in ^{159}Dy . In ^{157}Dy , the observed cross sections differ somewhat from the theoretical cross sections, but this is not unexpected as the couplings possible to $K\pi = 1/2 -$ and $K\pi = 3/2 -$ bands are numerous. The $3/2 -$ level at 399 keV is identified from the angular distribution and from energy systematics. The $5/2 -$ and $7/2 -$ states are observed at 454 keV and 527 keV, respectively.

In ^{159}Dy , the $3/2 -$ state is observed at 627 keV, the $5/2 -$ state at 690 keV, and the $7/2 -$ state at 774 keV. The observed cross sections are in reasonable agreement with theory. The $9/2 -$ triton group cannot be observed because of the presence of scattered deuterons.

2.3.7. The $1/2 - [530]$ Orbital

This orbital is characterized by the strong $3/2 -$ state and is expected at an excitation energy somewhat higher than that of the $1/2 + [400]$ state.

In ^{155}Dy , the $3/2 -$ state is observed at 381 keV and the levels at 422 keV and 482 keV are identified as the $5/2 -$ and $7/2 -$ states. The angular distrib-

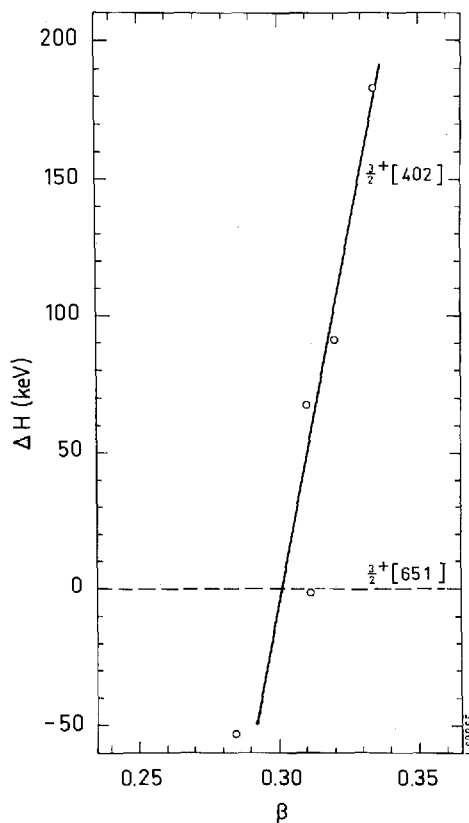


Fig. 20. Relative unperturbed energies of $3/2+ [402]$ and $3/2+ [651]$ as a function of the deformation.

utions and the intensity patterns are in reasonable agreement with this assignment.

In ^{157}Dy , the strong group at 555 keV is ascribed to the $3/2\ 1/2 - [530]$ state although it is stronger than expected. The only levels with a cross section greater than $5\ \mu\text{b/sr}$ are those at 565 keV and 673 keV. The level at 565 keV appears as a tail on the strong level at 555 keV, so the cross section is difficult to determine, but the level at 673 keV is relatively strong and has an angular distribution compatible with $l = 3$. If we assume that the two levels at 565 keV and 673 keV are the $5/2\ 1/2 - [530]$ and the $7/2\ 1/2 - [530]$ states, respectively, we get the band parameters $A = 8.7\ \text{keV}$ and $a = 0.77$. The decoupling parameter a is greater than in most other cases where the $1/2 - [530]$ orbital is identified. Another possibility is that the cross section of the $5/2 -$ state is less than $\sim 5\ \mu\text{b/sr}$ and is hidden in the background

TABLE 10. (d,t) population of $N = 6$ states.
 $d\sigma/d\Omega$, $\theta = 90^\circ$, $Q = -2$ MeV.

Spin	Theory	155	157	159	161	163	165
9/2			152	~ 80	~ 40	71	
13/2			50	~ 100	77	2 \sim 80	

TABLE 11. (d,t) population of the $5/2 - [523]$ band.

Spin	$d\sigma/d\Omega$, $\theta = 90^\circ$, $Q = -2$ MeV							Relative values of C_{Jt}^2						
	Theory	155	157	159	161	163	165	Theory	155	157	159	161	163	165
5/2	47		53	22	22	38		0.07		0.05	0.16	0.09	0.11	
7/2	48		95	55	43*	31		0.08		0.10	0.41	0.17	0.09	
9/2	55		132**	9	30	33		0.79		0.85	0.43	0.74	0.60	
11/2	4					11		0.06					0.20	
13/2														

* 9/2, 5/2 + [642] not resolved from this level, estimated contribution 51 % from theoretical cross sections.

** Coincides with 3/2 1/2 - [521]. From comparison with the (d,t) cross section of 1/2 1/2 - [521], the 3/2 1/2 - [521] (d,t) cross section is estimated to $\sim 12 \mu\text{b/sr}$.

TABLE 12. (d,t) population of the $11/2 - [505]$ band.
 $d\sigma/d\Omega$, $\theta = 90^\circ$, $Q = -2$ MeV.

Spin	Theory	155	157	159	161	163	165
11/2	88	62	71	82	79	70	

TABLE 13. (d,t) population of the $N = 4$ states.
 $d\sigma/d\Omega$, $\theta = 90^\circ$, $Q = -2$ MeV.

Level	Theory	155	157	159	161	163	165
3/2, 3/2 + [402]*	644	1054	778	694	712	700	
1/2, 1/2 + [400]*	819	786	846	834	947	582	
7/2, 7/2 + [404]	148				245	162	

* The table refers to the summed cross sections. See sects. 2.3.3 and 2.3.4.

which is seen in the spectra around 600 keV of excitation energy. In any case, the $1/2 - [530]$ orbital is distorted in the ^{157}Dy nucleus.

In ^{159}Dy , the $3/2\ 1/2 - [530]$ state is observed at 749 keV, the identification is based on the strength of the cross section and the angular distribution. The $5/2 -$ state probably coincides with the $7/2\ 3/2 - [532]$ state at 774 keV, so the cross section cannot be determined accurately. The $7/2 -$ state is observed at 828 keV and has a cross section relative to the $3/2 -$ state which is compatible with the theoretical cross section pattern.

In ^{161}Dy , the level at 860 keV is assigned as the $3/2\ 1/2 - [530]$ state, the $5/2 -$ state and the $7/2 -$ states are observed at 877 keV and 958 keV, respectively. The angular distributions are reasonable, but the $5/2 -$ group is too strong.

In ^{163}Dy , the $1/2 - [530]$ orbital is again difficult to establish, but from the strength of the cross section, the angular distribution and the systematics of the excitation energies, the level at 1275 keV is a good candidate for the $3/2\ 1/2 - [530]$ state.

The $7/2 -$ state is observed at 1359 keV and the level at 1425 keV is tentatively assigned as the $9/2 -$ state although it is stronger than expected. None of the assignments made for the $1/2 - [530]$ band is entirely satisfactory, and a similar remark applies for the $3/2 - [532]$ band which never has been observed without distortions. It seems likely that the Coriolis coupling of these states is responsible for most of the deviations between experimental and theoretical cross section patterns.

2.3.8. The $7/2 + [404]$ Orbital

The $7/2 + [404]$ orbital is characterized by one strong line belonging to the $7/2 +$ state. It is observed in ^{161}Dy at 1416 keV and in ^{163}Dy at 1840 keV with angular distributions in agreement with an $l = 4$ assignment. In the lighter dysprosium nuclei, the triton spectra are obscured by scattered deuterons in the region where the $7/2 + [404]$ group is expected.

2.3.9. The $5/2 - [523]$ Orbital

The $5/2 - [523]$ orbital is a particle state in ^{157}Dy , and the band head is observed at 340 keV. The $7/2 -$ state which is observed at 418 keV has an intensity three times larger than expected from theory. Deviations from the intensity patterns have been observed for the $5/2 - [523]$ orbital in other cases, and are caused by Coriolis coupling to the near-lying $3/2 - [521]$ orbital. The $9/2 -$ state coincides with the $3/2\ 1/2 - [521]$ state at 517 keV and the cross section cannot be given exactly.

TABLE 14. (d,t) population of the $1/2 - [530]$ band.

Spin	$d\sigma/d\Omega, \theta = 90^\circ, Q = -2 \text{ MeV}$							Relative values of C_{jt}^2						
	Theory	155	157	159	161	163	165	Theory	155	157	159	161	163	165
1/2	10							0.01						
3/2	339	286	526	238	284	103		0.21	0.52	0.51	0.49	0.68		
5/2	33	52	62	$\sim 30^*$	50			0.06	0.15	0.17	0.23	0.16		
7/2	130	118	122	87	51	45		0.23	0.33	0.32	0.28	0.16		
9/2	30					30		0.35						
11/2	13							0.14						

* Coincides with $7/2 \ 3/2 - [532]$.TABLE 15. (d,p) population of the $3/2 - [521]$ band.

Spin	$d\sigma/d\Omega, \theta = 90^\circ, Q = +3 \text{ MeV}$						Relative values of C_{jt}^2					
	Theory	157	159	161	163	165	Theory	157	159	161	163	165
3/2	103	61	63	42	$\sim 10^{**}$		0.10	0.17	0.17	0.13	0.14	
5/2	~ 0	3		3	9			0.01	0.01	0.01	0.13	
7/2	332	157	165	169	33		0.53	0.70	0.72	0.84	0.73	
9/2	18	26	$\sim 22^*$	3			0.26	0.12	0.10	0.02		
11/2	8						0.11					

* Coincides with $9/2 \ 5/2 + [642]$. ** Coincides with $5/2 \ 1/2 - [521]$.TABLE 16. (d,p) population of the $5/2 - [523]$ band.

Spin	$d\sigma/d\Omega, \theta = 90^\circ, Q = +3 \text{ MeV}$						Relative values of C_{jt}^2					
	Theory	157	159	161	163	165	Theory	157	159	161	163	165
5/2	47	39	30	24	15		0.07	0.07	0.06	0.14	0.05	
7/2	48	150	103	$\sim 38^*$	25		0.08	0.28	0.22	0.22	0.08	
9/2	55	$\sim 40^{**}$	25	13	25		0.79	0.65	0.47	0.64	0.70	
11/2	4		13		6		0.06		0.25		0.17	
13/2												

* $9/2, 5/2 + [642]$ not resolved from this level. ** Coincides with $3/2, 1/2 - [521]$.

In ^{159}Dy , the $5/2 - [523]$ band head is observed at 309 keV, the $7/2 -$ and $9/2 -$ states at 395 keV and 506 keV, respectively. Also in this nucleus the $7/2 -$ state is much stronger than expected. The 635 keV level is tentatively assigned as the $11/2 -$ state.

The low-lying state at 26 keV in ^{161}Dy is assigned as the $5/2 - [523]$ band head. The $7/2 -$ state at 104 keV cannot be separated from the $9/2$ $5/2 + [642]$ state in this nucleus, but the summed cross section for the two states seems to indicate that the Coriolis coupling between the $5/2 - [523]$ and $3/2 - [521]$ orbitals is weaker than in ^{157}Dy and ^{159}Dy .

In ^{163}Dy , the $5/2 - [523]$ orbital, the ground state and the rotational states up to the $11/2 -$ state are observed. The experimental cross sections are in reasonable agreement with theory and with previous experiments⁶⁾.

2.3.10. The $7/2 + [633]$ Orbital

This orbital is observed in the two heaviest dysprosium nuclei only. All states except the $9/2 +$ and $13/2 +$ states are expected to be weakly populated.

In ^{163}Dy , $9/2 +$ and $13/2 +$ assignments are suggested for the 499 keV and 719 keV levels, respectively. The two levels have angular distributions which indicate high angular momenta, and occur in the spectrum at the excitation energy expected. The strength of the $13/2 +$ state relative to the $9/2 +$ state is, however, less than expected from theory and from comparison with other nuclei where the $7/2 + [633]$ orbital is observed. In this connection, the coupling to the $N = 6$ states discussed in sect. 2.3.2 should be kept in mind.

The $7/2 + [633]$ orbital forms the ground state in $^{165}\text{Dy}^{7-10)}$. Only at 60° the ground state is observed with a cross section of $\sim 2 \mu\text{b}/\text{sr}$. The $9/2 +$ state at 84 keV and the $13/2 +$ state at 308 keV have (d, p) cross sections well in accordance with the theoretical predictions.

2.3.11. The $1/2 - [521]$ Orbital

The $1/2 - [521]$ orbital is populated in all the dysprosium nuclei investigated except ^{155}Dy , which can be reached by the (d, t) reaction only. This orbital is characterized by a strong $1/2 -$ state. The $5/2 -$ and $7/2 -$ states have each about half the strength of the $1/2 -$ state.

In ^{157}Dy , the $1/2 -$ state is observed at 464 keV with an angular distribution which is typical of $l = 1$. The $3/2 -$ state coincides with the $9/2$ $5/2 - [523]$ state at 520 keV, and the $5/2 -$ state is identified at 553 keV from the angular distribution and the strength of the cross section. The strong hole state $3/2$ $1/2 - [530]$ is observed at 555 keV and probably con-

TABLE 17. (d,p) population of the $7/2 + [633]$ band.

Spin	$d\sigma/d\Omega, \theta = 90^\circ, Q = +3 \text{ MeV}$							Relative values of C_{Jl}^2						
	The- ory	155	157	159	161	163	165	The- ory	155	157	159	161	163	165
7/2	~ 0							0.001						
9/2	21					$\leq 37^*$	16	0.07					0.20	0.05
11/2	~ 1							0.02						
13/2	41					22	47	0.92					0.80	0.95

* Probably some contributions from $11/2 \ 11/2 - [505]$.TABLE 18. (d,p) population of the $1/2 - [521]$ band.

Spin	$d\sigma/d\Omega, \theta = 90^\circ, Q = +3 \text{ MeV}$						Relative values of C_{Jl}^2					
	Theory	157	159	161	163	165	Theory	157	159	161	163	165
1/2	245	151	195	164	143	186	0.25	0.34	0.34	0.37	0.30	0.37
3/2	24	~ 17	25	35	4	17	0.02	0.04	0.04	0.08	0.01	0.04
5/2	114	129	71	61	$\sim 69^{**}$	73	0.18	0.46	0.20	0.21	0.23	0.23
7/2	145	44	155	82	138	106	0.23	0.16	0.42	0.29	0.46	0.33
9/2	19			14		7	0.27			0.05		0.02
11/2	3					4	0.05					0.01

* Coincides with $9/2 \ 5/2 - [523]$.** Coincides with $3/2 \ 3/2 - [521]$.TABLE 19. (d,p) population of the $5/2 - [512]$ band.

Spin	$d\sigma/d\Omega, \theta = 90^\circ, Q = +3 \text{ MeV}$						Relative values of C_{Jl}^2					
	Theory	157	159	161	163	165	Theory	157	159	161	163	165
5/2	6						0.01					
7/2	493	70	100	291	336	236	0.79	0.51	0.50	0.70	0.79	0.69
9/2	10	8	11	14	10	6	0.14	0.49	0.50	0.30	0.21	0.16
11/2	4					6	0.06					0.15

tributes to the (d,p) cross section of the peak at 553 keV, which is too strong according to the theory. On the other hand, the $7/2 -$ state, which is observed at 670 keV, is weaker than expected.

In ^{159}Dy , the 533 keV level is identified as the $1/2 -$ state from the angular distribution and the strength of the cross section. The $3/2 -$ and $5/2 -$ states are observed at 586 keV and 621 keV, respectively. In this nucleus, the $7/2 -$ state at 744 keV is stronger than expected. The explanation might also

here be that the (d,p) contribution from the $3/2\ 1/2 - [530]$ state cannot be resolved from the $7/2 -$ state.

In ^{161}Dy , the $1/2 - [521]$ band head is observed at 370 keV with an angular distribution very similar to the previously identified $1/2\ 1/2 - [521]$ states. The Q -corrected cross section is also similar to those observed for the corresponding states in ^{157}Dy and ^{159}Dy . The two peaks at 421 keV and 451 keV are identified as belonging to the $3/2 -$ state and the $5/2 -$ state, respectively, with the $7/2 -$ state observed at 572 keV. The peaks at 634 keV and 808 keV are tentatively assumed to belong to the $9/2 -$ and $11/2 -$ states.

In ^{163}Dy , the $1/2 -$ state is placed at 350 keV. The identification of the $1/2 - [521]$ band in ^{163}Dy is less straightforward than in the other dysprosium nuclei investigated, and the orbital shows deviations both in the decoupling parameter a and the cross sections of the different members of the rotational band. The $3/2 -$ state at 388 keV is very weakly populated. The $5/2 -$ state is observed at 425 keV, but part of the strength probably stems from the $3/2\ 3/2 - [521]$ state. The $7/2 -$ state at 517 keV has a relatively large (d,p) cross section, and also an apparently large (d,t) cross section. The latter may, however, contain contributions from the $13/2 +$ state discussed in sect. 2.3.2.

In ^{165}Dy , the $1/2 - [521]$ state is a low-lying particle excitation where the band head is observed at 109 keV. The angular distribution fits well into the pattern of the previously observed $1/2\ 1/2 - [521]$ states in the dysprosium nuclei. The $3/2 -$ state is observed at 158 keV, and the $5/2 -$ state at 182 keV. The rather strong peak at 298 keV is ascribed to the $7/2 -$ state, and also the $9/2 -$ and $11/2 -$ states give rise to weak peaks at 336 keV and 518 keV, respectively.

The $1/2 - [521]$ orbital has previously been identified at $^{161, 163, 165}\text{Dy}^{5-8)}$ and theoretical calculations of excitation energy, decoupling parameter and purity of the state have been performed for a number of nuclei, including $^{161, 163, 165}\text{Dy}$ by SOLOVIEV and VOGEL¹³⁾ and BÉs and CHO¹⁹⁾, taking into account the coupling between phonons and quasiparticles. The Coriolis coupling is not considered in these calculations. Especially in ^{163}Dy where the $3/2 - [521]$ orbital is close to the $1/2 - [521]$ orbital, this interaction is expected to be important.

The experimental values of the decoupling parameter a are collected in Table 21. Apart from the ^{163}Dy case, the variation in a is not more than 15%. This is in contrast to the theoretical values calculated by SOLOVIEV and VOGEL¹³⁾, which decrease a factor 2 from ^{165}Dy to ^{159}Dy .

2.3.12. The $5/2$ -[512] Orbital

The assignments made below are supported by the angular intensity variations, but represent only a fraction of the full theoretical intensity (cf. Table 19). The $5/2$ -[512] band is characterized by a strong $7/2$ - member.

In ^{157}Dy , the level is placed at 985 keV. The $9/2$ - state is tentatively assumed to be the one at 1101 keV.

In ^{159}Dy , the $7/2$ - state and $9/2$ - state are observed at 1089 keV and 1189 keV, respectively. The strong level at 1283 keV could be another choice for the $7/2$ - state, but the angular distribution makes the first assignment preferable.

In ^{161}Dy , the $7/2$ - state is observed at 883 keV. The $9/2$ - state is very likely the one at 995 keV, although the intensity is stronger than expected.

In ^{163}Dy , the level at 801 keV, which is strongly populated by the (d,p) reaction, is proposed to be the $7/2$ - state. The level at 918 keV possibly corresponds to the $9/2$ - state, although the rotational parameter is then larger than found in the other dysprosium nuclei.

In ^{165}Dy , the $5/2$ -[512] orbital is well established by previous work⁷⁻¹⁰⁾ as a low-lying particle state. The $7/2$ - state is observed at 262 keV and the $9/2$ - state at 361 keV. The band head coincides with the $5/2$ $1/2$ -[521] state at 182 keV.

From Table 19, it is seen that the strength of the $7/2$ $5/2$ -[512] state increases from ^{165}Dy to ^{163}Dy . This is in agreement with the decrease of pair occupation probability, V^2 , for the orbital concerned as neutrons are removed. In the lighter dysprosium nuclei, however, the strength decreases drastically, and the $7/2$ - cross section for ^{157}Dy is only 20% of that for ^{163}Dy .

Obviously the strength of the $7/2$ - states is split by some unknown interaction in the lighter dysprosium nuclei, where the excitation energy is comparatively high.

2.3.13. The $1/2$ -[510] Orbital

This orbital is expected to be a highly excited particle state in the Dy nuclei. The orbital is subject to strong particle-vibration interactions, giving rise to reduced cross sections and decoupling parameters less than the Nilsson value $a = -0.34$. The $3/2$ - state is strong and characteristic of the orbital.

In ^{157}Dy , the 1569 keV level is identified as $3/2$ - from the angular distribution and the cross section. The $5/2$ - and $7/2$ - states are observed at

TABLE 20. (d,p) population of the $1/2 - [510]$ band.

Spin	$d\sigma/d\Omega, \theta = 90^\circ, Q = 3 \text{ MeV}$						Relative values of C_{jl}^2					
	Theory	157	159	161	163	165	Theory	157	159	161	163	165
1/2	9				8		0.01				0.03	
3/2	398	62	84	148	171	138	0.41	0.45	0.57	0.60	0.54	0.70
5/2	183	17	19	42	62	28	0.29	0.19	0.20	0.27	0.30	0.22
7/2	120	32	21	21	27	9	0.19	0.36	0.23	0.13	0.13	0.08
9/2	6						0.09					
11/2	1						0.01					

TABLE 21. Decoupling parameters a for the $1/2 - [521]$ orbital.

	^{165}Dy	^{163}Dy	^{161}Dy	^{159}Dy	^{157}Dy
Experiment (this work).....	0.57	0.30	0.48	0.43	0.48
Theory (SOLOVIEV and VOGEL ¹³)..	0.86	0.60	0.47	0.42	

TABLE 22. Inertial parameters and decoupling parameters.
Number in brackets are decoupling parameters for $K = \frac{1}{2}$ bands.

Nilsson orbital	165	163	161	159	157	155
3/2 - [521]		10.6	11.5	11.4	12.0	10.9
5/2 - [523]		10.6	10.9	12.3	11.1	
5/2 + [642]		5.3	6.3	5.0		
1/2 + [660]		6.3(0.49)				
3/2 - [532]				12.6	11.0	
1/2 - [530]		7.0(-0.04)	7.5(0.55)	7.4(0.05)	8.7(0.77)	8.4(0.02)
1/2 - [521]	10.6(0.57)	10.0(0.30)	11.5(0.48)	12.3(0.43)	12.8(0.48)	
7/2 + [633]	9.3	9.2				
5/2 - [512]	11.1	13.0	12.4	11.1	12.9	
1/2 - [510]	11.2(0.036)	13.2(-0.048)	11.3(0.07)	12.4(-0.04)	11.2(-0.12)	
1/2 + [651]	9.1(0.03)		7.5(-0.15)			
3/2 - [512]	12.0	12.2				

1632 keV and 1701 keV, respectively. This assignment gives $A = 11.2$ keV and $a = 0.12$.

In ^{159}Dy , the $3/2 -$ state is observed at 1473 keV and the $5/2 -$ state at 1535 keV. The 1621 keV level has an angular distribution compatible with $l = 3$, and a $7/2 -$ assignment to this level gives the parameters $A = 12.4$ keV and $a = 0.04$.

In ^{161}Dy , the $3/2 -$ state is observed at 1309 keV, the $5/2 -$ state at 1363 keV and the $7/2 -$ state at 1446 keV. The parameters are here $A = 11.4$ keV and $\alpha = 0.049$.

In ^{163}Dy , the $3/2 -$ state is observed at 1199 keV with a large cross section. The $5/2 -$ and $7/2 -$ states are observed at 1262 keV and 1342 keV, respectively, and the weak level at 1159 keV is tentatively assigned to the $1/2 -$ state. These assignments correspond to the parameters $A = 12.0$ keV and $\alpha = 0.048$.

In ^{165}Dy , the $3/2\ 1/2 - [510]$ state is observed at 606 keV, which is significantly lower than in ^{163}Dy . The reduced cross section for the $3/2 -$ state at 90° is $138\ \mu\text{b/sr}$ as compared to $171\ \mu\text{b/sr}$ in ^{163}Dy . These facts indicate a stronger interaction between the $1/2 - [510]$ orbital and some vibrational mode than in the lighter dysprosium nuclei.

The theoretical predictions by SOLOVIEV and VOGEL¹³⁾ for the $1/2 - [510]$ orbital in ^{165}Dy are 32% $1/2 - [510]$, 63% gamma vibration based on $5/2 - [512]$ and 4% gamma vibration based on $3/2 - [512]$. The value of the decoupling parameter from SOLOVIEV and VOGEL's calculation is $\alpha = 0.05$, and from the calculation of BÉs and CHO¹⁹⁾ it is $\alpha = 0.03$. This is in good agreement with the experimental value $\alpha = 0.036$ which results from the identification of the $5/2 -$ state at 658 keV and the $7/2 -$ state at 737 keV. The inertial parameter is $A = 11.2$ keV.

2.3.14. The $3/2 - [512]$ Orbital

This orbital, which is observed in the three heaviest dysprosium nuclei, has a characteristic pattern consisting of a strong $5/2 -$ state and weaker $3/2 -$ and $7/2 -$ states.

The 1977 keV level in ^{161}Dy is assigned to the $3/2\ 3/2 - [512]$ state. The $5/2 -$ state is observed at 2039 keV, and the $7/2 -$ state is assumed to constitute the main part of an unresolved peak at 2113 keV. Both the angular distributions and the relative cross sections of the rotational band are compatible with the $3/2 - [512]$ assignment.

In ^{163}Dy , the $3/2 -$, $5/2 -$ and $7/2 -$ states are observed at 1795 keV, 1856 keV and 1936 keV, respectively. The angular distributions are typical of $l = 1$ and $l = 3$, but the cross section of the $5/2 -$ state is smaller than expected.

In ^{165}Dy , the $3/2 -$ state is placed at 1258 keV and $5/2 -$ and $7/2 -$ states at 1312 and 1402 keV, respectively. The assignments are based mainly on the angular distribution. Also in ^{165}Dy , the cross section of the $5/2 -$ state relative to the $3/2 -$ state and the $7/2 -$ state is smaller than expected. Com-

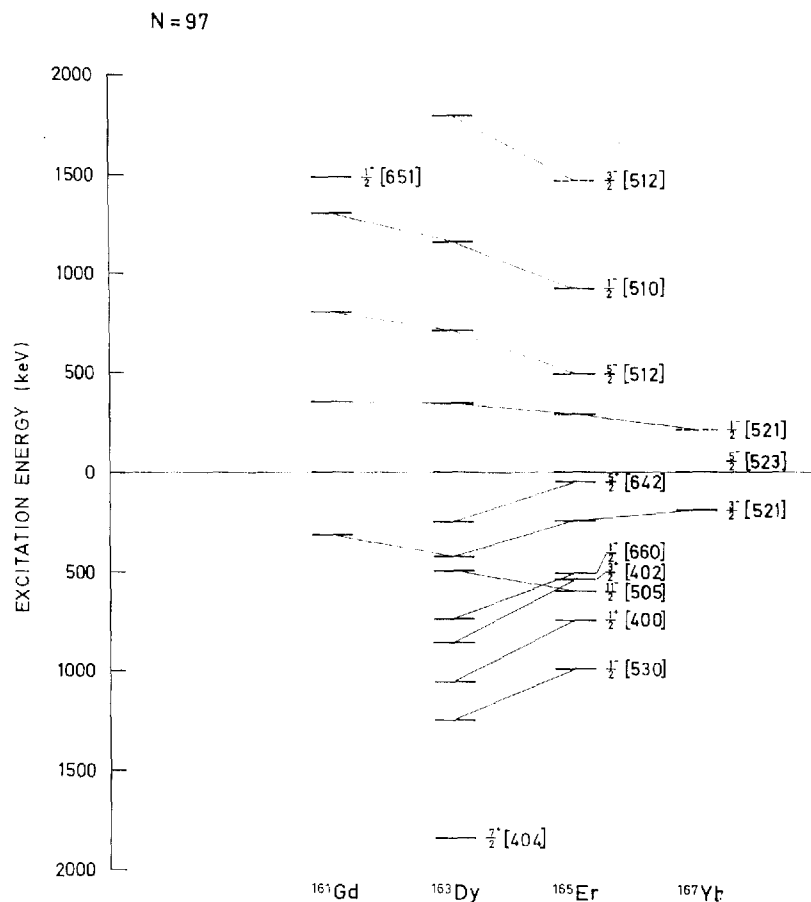


Fig. 21. Z-dependence of the band head energies for the isotones with $N = 97$.

pared to ^{163}Dy , the relative strengths of the members of the orbital are quite similar in the two nuclei, but the cross sections in ^{165}Dy are less than 50% of the cross sections in ^{163}Dy .

3. Z-Dependence of Single-Quasiparticle Energies

The number of single quasiparticle states identified in deformed nuclei has increased considerably during the later years. It is therefore possible to compare the single-quasiparticle energies of the same Nilsson state in several nuclei with the same number of neutrons. In all cases, except for

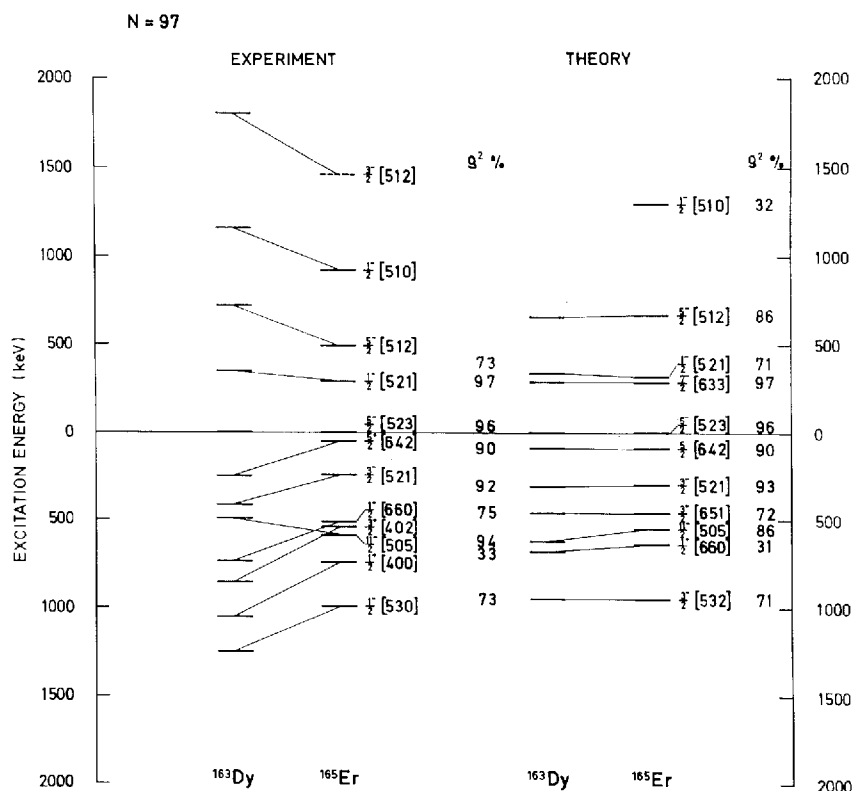


Fig. 22. Theoretical and experimental band head energies for ^{163}Dy and ^{165}Er .

neutron number 89, a systematic change in the band head energies is observed from one isotone to the next.

In Fig. 21, the band head energies of the identified Nilsson states are compared for the $N = 97$ isotones. The data for the gadolinium and erbium nuclei are mainly taken from refs. 1 and 2, the ytterbium data are taken from ref. 3.

The characteristic trend in this and other cases is the general compression or expansion of the band head energies as one goes from one isotone to the next. The few deviations from the pattern often concern orbitals which are affected by strong Coriolis coupling, such as, for instance, the $3/2 - [521]$ orbital in ^{161}Gd . Also the $11/2 - [505]$ orbital frequently shows an irregular behaviour.

Figure 22 gives a comparison with the theoretical calculations by SOLOVIEV et al.²⁰⁾, where the interactions between phonons and quasipar-

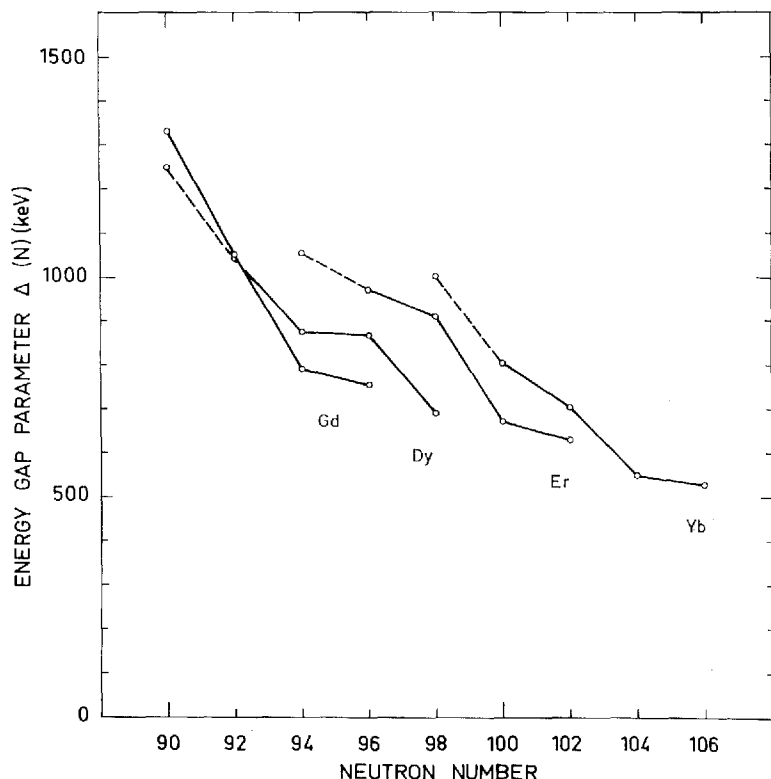


Fig. 23. The energy gap parameter $\Delta(N)$ for different elements as a function of the neutron number.

ticles are taken into account. The calculated energies agree well with the experimental energies for ^{165}Er , but the calculations do not reproduce the expansion in the observed excitation energies in ^{163}Dy .

The observed energies are the quasiparticle energies which, in the pairing formalism, are given by the expression

$$E_j = \sqrt{(\varepsilon_j - \lambda)^2 + \Delta^2} - \Delta, \quad (3)$$

where ε_j is the single-particle energy, λ the chemical potential, and Δ is the energy gap parameter for neutron orbitals.

It is experimentally known that the energy gap parameter Δ varies from element to element. The effect of this variation on the quasiparticle energies can easily be evaluated by Eq. (3) on the assumption of constant $(\varepsilon_j - \lambda)$. The energy gap parameter can be calculated from the neutron separation energies by the formula

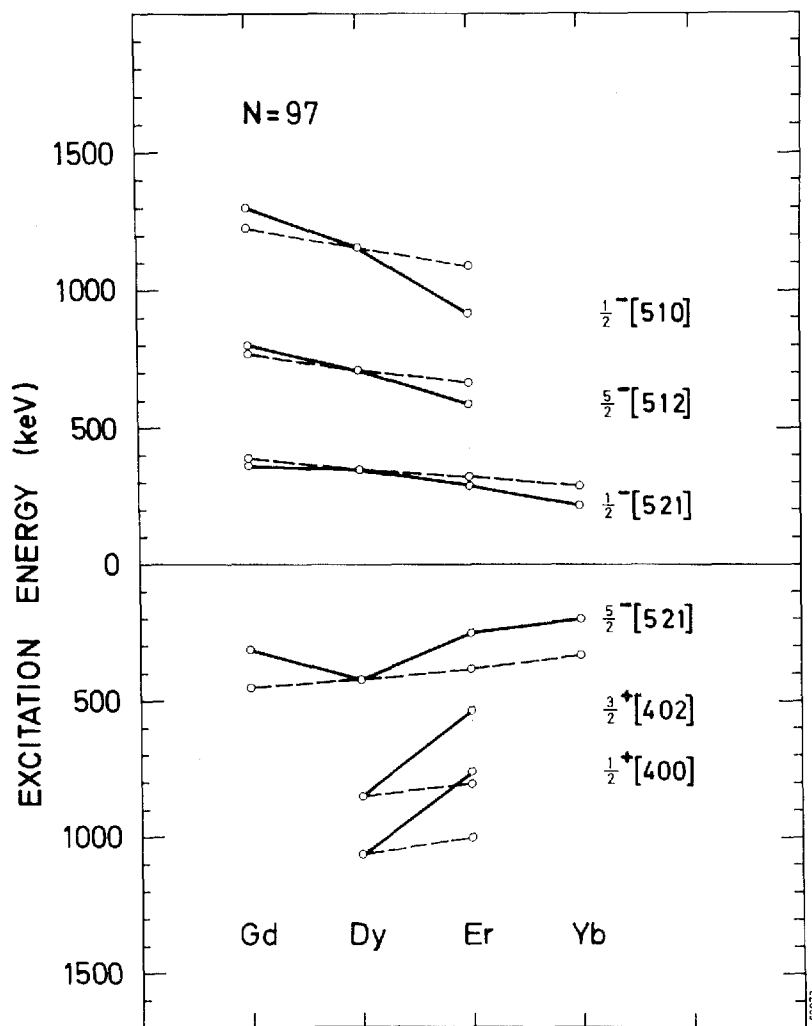


Fig. 24. The effect of Δ on the quasiparticle energies assuming a constant $(\epsilon - \lambda)$ normalized to the Dy case. The dotted lines show the calculated quasiparticle energies, the full lines the experimental energies.

$$\Delta(N) = 1/2[S_n(N) - S_n(N-1)], \quad (N \text{ even}) \quad (4)$$

where the experimental neutron separation energies for Gd, Er, and Yb are available^{1, 2, 3}). In Fig. 23, the variation of Δ versus the neutron number N is plotted for different elements. The calculated quasiparticle energies for $N = 97$ are shown in Fig. 24, where the observed excitation energies are connected by solid lines, whereas the calculated energies are connected

through dotted lines. The slope of the dotted lines shows the effect of Δ assuming a constant $(\epsilon_j - \lambda)$ normalized to the Dy case. It is clearly seen that only part of the observed energy shifts can be explained in this way.

The calculations by SOLOVIEV and VOGEL¹³⁾ show that the coupling to the gamma vibration affects the single-quasiparticle energies. As the energy and strength of the gamma vibration in the even nuclei, for a fixed neutron number, show some dependence on Z , part of the variation illustrated in Fig. 24 might be ascribed to particle-phonon coupling.

4. Summary

The present work has identified a total of 16 different Nilsson orbitals with their associated rotational bands.

The level order is almost identical to the one found in gadolinium, and again confirms the Nilsson scheme. It is also interesting to see how the inclusion of the phonon-quasiparticle interaction²⁰⁾ improves the overall agreement (Fig. 22). Some of the remaining discrepancies might have their origin in the Coriolis interaction which is not included in the model.

The Z -dependence of the neutron quasiparticle energies shows a remarkable symmetric pattern with few irregularities. The Z -dependent variation in the level density is more pronounced for the heavier nuclei than in the lighter ones. In the $N = 89$ isotones ^{153}Gd and ^{155}Dy , there is practically no change in the band head energies. If the particle-phonon interaction is included, the quasiparticle energies are compressed compared with the Nilsson scheme. The Z -dependent compression revealed by the data might partly be explained by a difference in the vibration strength from one isotope to another.

Acknowledgements

The authors want to thank IRENE JENSEN and RAGNHILD FAGERBAKKE for careful plate scanning. The targets were prepared by G. SØRENSEN, J. THORSAGER and V. TOFT at the University of Aarhus Isotope Separator. T. GROTDAL and K. NYBØ acknowledge support from Det Vitenskapelige Forskningsfond av 1919.

*The Niels Bohr Institute
University of Copenhagen*

*Institute of Physics
University of Bergen*

References

- 1) P. O. TJØM and B. ELBEK, Mat. Fys. Medd. Dan. Vid. Selsk. **36**, no. 8 (1967).
- 2) P. O. TJØM and B. ELBEK, Mat. Fys. Medd. Dan. Vid. Selsk. **37**, no. 7 (1969).
- 3) D. G. BURKE, B. ZEIDMAN, B. ELBEK, B. HERSKIND and M. C. OLESEN, Mat. Fys. Medd. Dan. Vid. Selsk. **35**, no. 2 (1966).
- 4) J. BORGGREEN and J. P. GJALDBÆK, Nucl. Phys. A **113** (1968) 659.
- 5) L. FUNKE, H. GRUBER, K.-H. KUNN, J. RÖMER and H. SODAN, Nucl. Phys. **84** (1966) 443.
- 6) O. W. B. SCHULT et al., Phys. Rev. **154** (1967) 1146.
- 7) R. K. SHELINE and H. T. MOTZ, Phys. Rev. **136** (1964) B 351.
- 8) O. W. B. SCHULT, B. P. MAIER and U. GRUBER, Z. Phys. **182** (1964) 171.
- 9) G. MARKUS, W. MICHAELIS, H. SCHMIDT and C. WEITKAMP, Z. Phys. **206** (1967) 84.
- 10) B. C. DUTTA, T. V. EGIDY, TH. W. ELZE and W. KAISER, Z. Phys. **207** (1967) 153.
- 11) S. SJØFLOT and T. SILNES, private communication.
- 12) J. H. E. MATTAUCH, W. THIELE and A. H. WAPSTRA, Nucl. Phys. **67** (1965) 1.
- 13) V. G. SOLOVIEV and P. VOGEL, Nucl. Phys. A **92** (1967) 449.
- 14) J. BORGGREEN, G. LØVHØIDEN and J. C. WADDINGTON, Nucl. Phys. A **131** (1969) 241.
- 15) M. JASKOLA, P. O. TJØM and B. ELBEK, Nucl. Phys. A **133** (1969) 65.
- 16) B. L. ANDERSEN, Nucl. Phys. A **112** (1968) 443.
- 17) G. LØVHØIDEN, private communication.
- 18) L. FUNKE et al., Nucl. Phys. **55** (1964) 401.
- 19) D. R. BÉS and CHO YI CHUNG, Nucl. Phys. **86** (1966) 581.
- 20) V. G. SOLOVIEV, P. VOGEL and G. JUNGCLAUSSEN, Izv. Akad. Nauk, USSR, Ser. fiz. **31** (1967) 518.

